[redacted]

Copy
RM L53I08

[redacted]

NACA

RESEARCH MEMORANDUM

AERODYNAMIC CHARACTERISTICS OF A 68.4° DELTA WING AT MACH NUMBERS OF 1.6 AND 1.9 OVER A WIDE REYNOLDS NUMBER RANGE

By John E. Hatch, Jr., and James J. Gallagher

Langley Aeronautical Laboratory
Langley Field, Va.

NATIONAL ADVISORY COMMITTEE
FOR AERONAUTICS

WASHINGTON

November 2, 1953

[redacted]

[redacted]

Classification cancelled (or changed to UNCLASSIFIED)

By Authority of List + Tech Pub Announcement #67
(OFFICER AUTHORIZED TO CHANGE)

By ..... NAME AND

GRADE OF OFFICER MAKING CHANGE)

4 Apr 61

DATE

.Q

NACA RM L53I08 [redacted]

NATIONAL ADVISORY COMMITTEE FOR AERONAUTICS

RESEARCH MEMORANDUM

AERODYNAMIC CHARACTERISTICS OF A 68.4° DELTA WING AT MACH NUMBERS OF 1.6 AND 1.9 OVER A WIDE REYNOLDS NUMBER RANGE

By John E. Hatch, Jr., and James J. Gallagher

SUMMARY

The results of an experimental investigation to determine the effects of Reynolds number on the aerodynamic characteristics of a 68.4° delta wing at Mach numbers of 1.6 and 1.9 are presented. The wing streamwise airfoil sections are based on the NACA 00-series with the maximum thickness varying from 4 percent at the root section to 6.24 percent at the 90-percent semispan station. At a Mach number of 1.90 force and pressure data were obtained over an angle-of-attack range of 16° at Reynolds numbers of 7.2×10^6, 12.6×10^6, and 18.4×10^6. Pressure data were also obtained at Mach numbers of 1.93 and 1.62 at Reynolds numbers of 2.2×10^6 and 7.4×10^6 up to an angle of attack of 10°.

At Mach number 1.90 the force data indicated that Reynolds number had no significant effects on the measured lift and pitching moment. As the Reynolds number increased from 7.2×10^6 to 18.4×10^6, however, the minimum drag coefficient of the wing (largely turbulent boundary layer) decreased approximately 8 percent. For the same Reynolds number range there was no change in the amount of leading-edge suction developed by the wing which was approximately 15 percent of the theoretical value.

At a given angle of attack the pressure data obtained at Mach numbers of 1.9 and 1.62 showed that an increase in Reynolds number affected the magnitude and distribution of chordwise loading but had little effect on the spanwise loading.

At both test Mach numbers the shape of the spanwise loading curve varied from elliptical at the low angles of attack to more nearly triangular at the higher angles.

[redacted]

[redacted]

INTRODUCTION

The effects of a large change in Reynolds number on the aerodynamic characteristics of a 68.4° delta wing at a Mach number of 2.41 have been reported in reference 1. The greatest effect of an increase in Reynolds number from 1.04×10^6 to 18.3×10^6 was to vary the pressure distribution over the wing upper surface at angle of attack. It was shown that an increase in Reynolds number delayed to a higher angle of attack the formation of a separated region near the wing leading edge. This region terminated in a shock wave lying approximately on a ray through the wing apex.

The purpose of the present paper is to provide further information on the effects of Reynolds number on the aerodynamic characteristics of the wing of reference 1 as well as to provide load distributions for the wing at Mach numbers of 1.6 and 1.9.

Flow-direction surveys on the wing upper surface were made in order to provide additional information on the flow phenomena over the wing.

SYMBOLS

Free-stream conditions:

M	Mach number
q_o	dynamic pressure
p_o	static pressure
R	Reynolds number, based on wing mean aerodynamic chord

Wing geometry:

A	aspect ratio
b	span
C	tangent of apex angle
c	wing chord, measured in direction of flight
$\bar{c}$	mean aerodynamic chord

[redacted]

c_{av}	average chord
S	wing area
t	thickness
α	angle of attack, deg
x	coordinate along free-stream direction
y	spanwise coordinate

Pressure data:

p	local static pressure
C_p	pressure coefficient, $\frac{p - p_o}{q_o}$
$\frac{\Delta p}{q_o \alpha}$	lifting-surface pressure coefficient per degree angle of attack, $\frac{p_l - p_u}{q_o \alpha}$
$\frac{c_n c}{c_{av}}$	span-loading coefficient, $\int_0^c \frac{C_{p_l} - C_{p_u}}{c_{av}} dc$
ψ	local flow angle

Force data:

C_L	wing-lift coefficient, $\frac{\text{Lift}}{q_o S}$
C_D	wing-drag coefficient, $\frac{\text{Drag}}{q_o S}$
C_M	wing pitching-moment coefficient about wing centroid of area, $\frac{\text{Pitching moment}}{q_o S \bar{c}}$
C_c	chord-force coefficient, $\frac{\text{Chord force}}{q_o S}$

$\frac{L}{D}$ lift-drag ratio

F_s theoretical suction force coefficient, $\frac{C_L^2}{\pi A}\sqrt{1 - \beta^2 C^2}$

$\beta = \sqrt{M^2 - 1}$

ΔC_D incremental drag coefficient due to lift, $C_D - C_{D_{min}}$

Subscripts:

u conditions on wing upper surface

l conditions on wing lower surface

r value at root section

max maximum value

min minimum value

APPARATUS

Blowdown jet.- The high Reynolds number tests at $M = 1.90$ were conducted in one of the 9-inch blowdown jets of the Gas Dynamics Branch at the Langley Laboratory. The jet was so designed that the semispan models could be mounted with or without a boundary-layer scoop (fig. 1). The test section was 9 inches wide and 6 inches high when the scoop was used and 9 inches wide and 6.75 inches high when the scoop was removed.

Tunnel.- The low Reynolds number tests at $M = 1.62$ and $M = 1.93$ were conducted in the Langley 9-inch supersonic tunnel. This tunnel is a single-return, direct-drive type in which the pressure, temperature, and humidity of the enclosed air can be controlled. The semispan-wing models were mounted directly to the tunnel sidewall with no tunnel boundary-layer scoop.

Models.- The semispan-wing models having an aspect ratio of 1.57 were constructed from steel. Streamwise airfoil sections are based on the NACA 00-thickness series which has its maximum thickness at 30 percent of the chord. Leading-edge radii were modified to average about 0.4 percent of the local chord. The measured wing maximum thickness varied from

4 percent at the root to 6.24 percent at the 90-percent semispan station as shown in figure 2(a). A sketch of the wing showing the locations of the pressure-survey stations is shown in figure 2(b), and the chordwise orifice locations are given in table II. Two pressure-distribution models were used in order to include the desired number of orifices, and another similar model was used for the force tests.

In order to determine the local flow direction over the wing upper surface at angles of attack, small, symmetrical, weathercocking vanes were installed on a full-span sting-mounted model in the 9-inch supersonic tunnel. Figure 3 shows the physical dimensions of the vanes as well as the vane locations on the wing surface.

TESTS AND PRECISION

The following table shows the range of the tests and the facilities used during the present investigation.

Facility	M	R	α	Data obtained
Langley 9-inch supersonic tunnel	1.62	2.2×10^6	0° to 10°	Pressure distributions
	1.62	7.2×10^6	0° to 10°	
	1.93	2.2×10^6	0° to 10°	Pressure distributions
	1.93	7.2×10^6	0° to 10°	
Blowdown jet of the Langley Gas Dynamics Branch	1.90	7.2×10^6	0° to 16°	Pressure distributions and forces
	1.90	12.6×10^6	0° to 16°	
	1.90	18.4×10^6	0° to 16°	

The wing was tested in a blowdown jet with and without a boundary-layer scoop. Force data and pressure distributions indicated practically no differences in the aerodynamic characteristics of the wing as determined by the two methods of testing. (See appendix.) The data presented for the wing, therefore, are the results obtained from the wall-mounted model with no tunnel boundary-layer scoop.

The turbulence level in the Langley 9-inch supersonic tunnel is known to be relatively low (ref. 2) and extensive laminar boundary layers are found under some conditions. In the blowdown jet, however, the turbulence level is unknown but is believed to be relatively high; this level probably results in the model boundary layers being largely turbulent for all test Reynolds numbers in this facility.

[redacted]

In order to understand better the direction of air flow over the wing surface, small vanes were installed at 16 different locations on the full-span model in the Langley 9-inch supersonic tunnel. The vanes were so located on the wing during each run that no interference effects between vanes were possible.

The angles through which the vanes were turned at each wing angle of attack were read by means of a cathetometer mounted outside of the tunnel. The accuracy of measurement of the indicated flow angles is estimated at $\pm\frac{1}{2}^{\circ}$. Additional information on the direction of flow in the boundary layer was obtained by an ink-flow method. Ink was allowed to issue from the wing surface through static orifices located in the wing, and the path of the ink taken in the boundary layer was photographed.

The estimated probable errors in the aerodynamic coefficients are as follows:

R	C_p	C_L	C_D	C_M	C_c ($\alpha = 0$)
2.2×10^6	±0.0050	-------	-------	-------	-------
7.2×10^6	±0.0015	±0.0020	±0.0006	±0.0006	±0.0002
12.6×10^6	±0.0030	±0.0010	±0.0003	±0.0003	±0.0001
18.4×10^6	±0.0020	±0.0020	±0.0003	±0.0003	±0.0001

Calibration of the tunnel shows the Mach number to be 1.62 ± 0.01 and 1.93 ± 0.015. For the blowdown jet the Mach number was 1.90 ± 0.015. The probable error in angle of attack in referencing the models was ±0.07° with respect to the tunnel center line and ±0.03° in relative angle of attack.

RESULTS AND DISCUSSION

Force Data

The force data were obtained only with the semispan model in the blowdown jet at $M = 1.90$. Data are presented in figure 4 at Reynolds numbers of 7.2×10^6 and 18.4×10^6 based on the mean aerodynamic chord. Force data taken at a $R = 12.6 \times 10^6$ were the same as those obtained at $R = 18.4 \times 10^6$ and, therefore, are not presented.

Lift.- No significant effects within the experimental accuracy can be noted on the lift throughout the range of Reynolds numbers tested. The lift-curve slope is linear up to about an angle of attack of 8° where the slope begins to decrease because of separation effects. For the low angles of attack the slope of the lift curve was 0.0290 per degree compared to the value of 0.033 as obtained from theory in reference 3.

Drag.- The only significant change in the drag data with Reynolds number was a variation of $C_{D_{min}}$. A value of $C_{D_{min}}$ of 0.0094 was obtained at a Reynolds number of 7.2×10^{6} and decreased to 0.0086 at a Reynolds number of 18.4×10^{6}. Up to about an angle of attack of 8° a slight decrease in drag coefficient with increasing Reynolds number may also be noted. It is believed that the wing boundary layer is almost entirely turbulent at the test Reynolds numbers, and a decrease of this order of magnitude in drag coefficient is to be expected with increasing Reynolds number.

Integration of the pressure distributions obtained at a Reynolds number of 18.4×10^{6} (fig. 5) gives a value of 0.0051 for the pressure drag coefficient for this wing. When the pressure drag coefficient is subtracted from $C_{D_{min}}$ for the wing mounted on the sidewall, a value of 0.0035 for the skin-friction coefficient is obtained at a Reynolds number of 18.4×10^{6}. For the wing in the presence of the boundary-layer scoop the skin-friction coefficient was found to be 0.0040. For a flat plate at the same Reynolds number, reference 4 gives an experimental value of 0.0044 for the turbulent skin-friction coefficient; this value compares favorably with that obtained for the wing.

Lift-drag ratio.- A value of 7.2 for $(L/D)_{max}$ is obtained at the highest Reynolds number. This value decreases slightly with decreasing Reynolds number; this decrease is due in part to the increase in skin friction obtained at the lower Reynolds numbers.

Pitching moment.- The only discernible Reynolds number effects appear in the pitching moment although even these are small. Figure 4 shows that at the higher angles of attack the center of pressure of the wing moves forward slightly with increasing Reynolds number. The shift amounts to a forward movement of the center of pressure of about only 1 percent of the mean aerodynamic chord at an angle of attack of 16°. The reversal in slope in the moment curve at about an angle of attack of 8° coincides with the point at which the lift-curve slope begins to decrease.

Leading-edge suction.- The linearized theory predicts that a suction force is developed on round-nose airfoils at supersonic speeds when the leading edge of the airfoil is swept behind the Mach cone. When the value

of the drag-rise factor $\Delta C_D/C_L^2$ is less than the reciprocal of the lift-curve slope, a suction force is developed which indicates that the resultant lift vector is tilted forward. Experimentally, a decrease in skin friction with increasing angle of attack would also show the same effect. Since it is not possible to isolate completely the skin-friction effects on the drag-rise factor, the concept of leading-edge suction should be used only as a convenient method of comparing the relative merits of different wings.

Figure 6 shows the experimental variation of ΔC_D with C_L^2 as well as the theoretical curve assuming the wing to be developing full leading-edge suction. Only about 15 percent of the theoretical suction force was indicated. Although the data are not shown, a change in Reynolds number from 7.2×10^6 to 18.4×10^6 had no effect on the leading-edge suction for this wing. Figure 7 is presented in order to show more clearly the little drag relief that was obtained. The theoretical chord-force coefficient, assuming the wing to be developing full leading-edge suction, was calculated by the method of reference 2 by using the theoretical lift-curve slope for the wing. The theoretical curve if extended indicates that the wing would actually have a negative value of chord-force coefficient at an angle of attack above 5° if full suction were attained. Actually, of course, the leading-edge-suction force is limited to some value of pressure close to vacuum acting on a small area along the leading edge. The experimental curve does show a decrease in C_c but it is nowhere near the order predicted by theory.

FLOW STUDIES

An examination of the pressure data indicated that the character of the flow over the wing is, in general, the same at $M = 1.6$ and 1.9 as it was at $M = 2.41$ (ref. 1). Pressure discontinuities on the wing upper surface show that standing shock waves exist at each of the test Mach numbers. For example, figure 8 shows the spanwise variation of upper-surface pressure coefficients at the 90-percent root-chord station for a wing angle of attack of 10° at $M = 1.9$. The data at each Reynolds number indicate that a separated region exists near the leading edge and is followed by an abrupt change in pressure which usually denotes the presence of a shock wave. From additional spanwise pressure plots, the shock wave was found to lie along a ray through the wing apex.

A flow-direction survey was made just above the wing surface by means of weathercocking vanes placed on the full-span wing. In addition, the flow direction in the boundary layer was observed by means of an ink-flow technique. From the results of the vane survey, it was found that outboard

of the shock wave lying along a ray through the wing apex the flow was toward the root chord, whereas, behind the shock wave, the flow was approximately parallel to the root chord. Figure 9 shows some results of the flow-direction survey made at the 70-percent root chord station. At $M = 1.62$ and $M = 1.93$, the local flow angles increased with increasing angle of attack. It should be noted that the abrupt change in the indicated flow angles occurs at the location of the shock wave on the wing surface as determined from the pressure distributions. Complete results of the vane survey are presented in table I.

The flow direction in the boundary layer was observed at $M = 1.93$ in the Langley 9-inch supersonic tunnel over an angle-of-attack range as the Reynolds number varied from 1.3×10^6 to 5×10^6. Ink was admitted at several points on the full-span wing upper surface and the resulting flow patterns were photographed as the angle of attack and Reynolds number were varied. Figure 10 shows some results of the ink-flow studies obtained at a Reynolds number of 1.3×10^6 over an angle-of-attack range. With the wing at an angle of attack of 0° the ink flowed approximately parallel to the stream direction, but, as the angle of attack increased, the ink showed that the boundary-layer flow at the wing surface was turned outboard and toward the tip. The ink-flow pictures as well as the pressure data show that separation begins at the tip and moves toward the wing apex with increasing angle of attack. Combining the results of pressure distributions, vane surveys, and the ink-flow photographs led to the conclusion that the flow configuration was probably as shown in figure 11. A lambda shock occurred on the wing with the front leg starting at the point of laminar separation and the back leg originating along the line of flow reattachment. Between the two legs of the lambda shock the flow direction was outboard on the wing surface and inboard a small distance above the surface. Behind the back leg of the lambda shock the flow just above the surface is approximately parallel to the stream direction as shown by the vane survey. Similar wing-shock configurations were photographed and reported in reference 5.

Pressure data obtained at a Reynolds number of 18.4×10^6 show that up to an angle of attack of 16° (the limit of the present tests) the back leg of the lambda shock moves inboard and the leading-edge separation continues to move toward the wing apex with increasing angle of attack.

Figure 12 shows some ink-flow pictures for the wing at an angle of attack of 2° as the Reynolds number was varied from 1.3×10^6 to 5×10^6 at $M = 1.93$. At a Reynolds number of 1.3×10^6, the ink-flow photographs indicate that separation has started near the tip as evidenced by the ink flowing along the leading edge. As the Reynolds number is increased the point of leading-edge separation moves toward the tip until finally the ink spreads out over the wing surface and then flows in the stream direction

which shows that the flow is no longer separated. The pressure-distribution data also indicate that an increase in Reynolds number delays the leading-edge separation to a higher angle of attack.

LOADING

It has been shown that an increase in test Reynolds number changes the flow over the wing. It will, therefore, be of interest to determine the effect that Reynolds number has on the wing loading coefficients. Only representative data which show the effects of Reynolds number are plotted in this paper. Complete pressure data for the wing at $M = 1.62$ and $M = 1.9$ are presented in tables II and III.

Figure 13(a) shows the chordwise variation of loading coefficients for the wing at $M = 1.9$ and $\alpha = 6^{\circ}$ for Reynolds numbers of 2.2×10^6 and 18.4×10^6. At the 11.1-percent semispan station there is little effect of Reynolds number on the loading, but in moving outboard the distribution and magnitude of the chordwise loading coefficients change with Reynolds number. For example, at the 77.7-percent semispan station the higher Reynolds number tests result in loading coefficients on the order of 15 to 20 percent higher than those obtained at a Reyonolds number of 2.2×10^6. The agreement between experiment and theory is good at the inboard station, but becomes progressively worse in moving outboard owing to flow separation which begins at the tip. As a result of flow separation the loading over the three outboard stations is not linear with angle of attack. The variation in loading at the inboard station, however, is nearly linear over the entire test range.

It was found that the greatest changes in loading coefficients occurred as the Reynolds number was increased from 2.2×10^6 to 7.2×10^6. As the Reynolds number was further increased to 18.4×10^6 the loading continued to vary but the changes in loading over that obtained at a Reynolds number 7.2×10^6 were small. As the angle of attack increased above 6° the effects of Reynolds number on the chordwise loading coefficients decreased. The pressure data indicate that at about an angle of attack of 14° Reynolds number will have little effect on the loading coefficients since the flow has separated over most of the wing even at a Reynolds number of 18.4×10^6. The pressure-distribution data obtained at a Reynolds number of 7.2×10^6 in the Langley 9-inch supersonic tunnel at angles of attack up to 10° (the limit of the tunnel tests) were in good agreement with those data (not presented) for the wing at the same Reynolds number in the blowdown jet.

As shown by figure 13(b) the same general changes in wing loading occurred with Reynolds number at $M = 1.62$ as occurred at $M = 1.9$. Even though the highest test Reynolds number at $M = 1.62$ was 7.2×10^6 it is believed that the loading coefficients presented are approximately the same as would be obtained at higher Reynolds numbers since at $M = 1.9$ and $M = 2.41$ an increase in Reynolds number above 7.2×10^6 had little effect on the wing loading coefficients.

Figure 13 illustrated that Reynolds number had significant effects on the distribution and magnitude of chordwise loading coefficients. It is important, then, to examine the effects of Reynolds number on the spanwise loading which was obtained from the integrated pressure distributions at each chordwise station.

Figure 14(a) shows the variation in experimental loading across the span for the wing at angles of attack of 6°, 10°, and 16° at $M = 1.9$. It may be seen that the effects of Reynolds number on the spanwise loading are small. At an angle of attack of 6°, for example, the integrated data obtained at a Reynolds number of 18.4×10^6 result in a lift coefficient approximately 4 percent higher than the lift coefficient obtained at a Reynolds number of 2.2×10^6. The experimental data and theory show good agreement at an angle of attack of 6°. As the angle of attack increases to 16° the shape of the span-loading curve changes from near elliptical to approximately a triangular distribution. Figure 14(b) shows that the span loadings at $M = 1.62$ also follow the same trends.

CONCLUSIONS

From the experimental investigation to determine the effects of Reynolds number on the aerodynamic characteristics of a delta wing the following conclusions may be drawn:

1. Over an angle-of-attack range of 0° to 16° at Mach number 1.90 the only significant effect of a Reynolds number change from 7.2×10^6 to 18.4×10^6 on the measured force data was to decrease the wing minimum drag coefficient about 8 percent.

2. At Mach number 1.90, there was no effect of a Reynolds number increase from 7.2×10^6 to 18.4×10^6 on the amount of leading-edge suction developed by the wing which was approximately 15 percent of the theoretical value.

3. At Mach numbers 1.62 and 1.9, a large increase in Reynolds number definitely affected the magnitude and distribution of chordwise loading but had little effect on the resultant spanwise loading.

4. The shape of the spanwise loading curve varied from elliptical at the low angles of attack to more nearly triangular at the higher angles.

5. With the semispan wing mounted directly to the tunnel side wall at Mach numbers 1.90 and 2.41, the wing aerodynamic characteristics were the same as those obtained with the wing tested in the presence of a tunnel boundary-layer scoop for Reynolds numbers of 12.6×10^6 and 18.4×10^6.

Langley Aeronautical Laboratory,
National Advisory Committee for Aeronautics,
Langley Field, Va., August 25, 1953.

APPENDIX

The use of a boundary-layer scoop exhausting to the atmosphere presents several problems. For example, the scoop will not start at low stagnation pressure which, of course, means that low Reynolds number tests cannot be made. In addition, a disturbance which is not always easily eliminated originates from the scoop—tunnel-wall juncture. It would be desirable and convenient, therefore, to conduct tests at supersonic speeds without a boundary-layer scoop if the test results would not be adversely affected.

During the present investigation, the effects of testing a 68.4° delta wing with and without a boundary-layer scoop were determined. The ratio of the tunnel boundary-layer thickness to wing semispan was about 1/10 when the wing was tested without the boundary-layer scoop.

Force test.- Figure 15 shows force data obtained at $M = 1.90$ and $M = 2.41$ for the wing tested with and without a boundary-layer scoop. Up to an angle of attack of 16° (the limit of the present tests), the only significant effect on the measured force coefficients of testing the wing mounted directly to the side wall was to lower the minimum drag coefficient approximately 3 to 5 percent. A small decrease in drag coefficient is to be expected since part of the wing was immersed in the tunnel boundary layer. At $M = 2.41$ there was a slight rearward shift in the wing center-of-pressure location when the wing was tested without a boundary-layer scoop in place. At an angle of attack of 16° the rearward center-of-pressure shift was about 1 percent of the mean aerodynamic chord.

Pressure data.- For the no-scoop condition, if the tunnel boundary layer were to influence the pressure distribution over the wing, the pressures at the inboard stations would be most affected. Figure 16 presents representative plots of pressure coefficients at the 11.1-percent semispan station for $M = 1.9$ and a Reynolds number of 18.4×10^{6}. Figure 16 shows that the pressure data obtained by the two methods of testing are the same. The agreement shown at the inboard station is typical of the pressure distributions at the other spanwise stations over the test angle-of-attack range of 0° to 16°.

Figure 17 shows some typical pressure distributions at $M = 2.41$ for the 11.1-percent and 33.3-percent semispan stations. At the 11.1-percent semispan station the pressures show some disagreement over the forward 40 percent of the airfoil between the two methods of testing. At angles of attack, the scoop tests result in slightly higher negative pressures on the upper surface than do the no-scoop tests. The trends, which occurred at $\alpha = 8^{\circ}$, continued to the higher angles of attack, but the agreement was somewhat improved at the higher angles.

At the 33.3-percent semispan station the pressures obtained show good agreement over the forward 60 percent of the airfoil at $\alpha = 0^\circ$, but over the remainder of the airfoil the scoop tests again result in higher negative pressures than those pressures obtained without the boundary-layer scoop. When the angle of attack is increased to 8°, no differences in the pressure distributions are noticeable. The pressures obtained at the 55.5-percent and the 77.7-percent semispan stations were the same for both methods of testing over the angle-of-attack range of 0° to 16°.

It may be seen, therefore, that the no-scoop tests result in local decreases in lifting pressures on the order to 5 percent below the pressures obtained with a scoop-mounted model. The local reductions in lift are also apparent in the force data which indicated a slight rearward shift in the center of pressure for the no-scoop tests.

The results of the present tests indicate that, when testing highly sweptback wings at Mach numbers of about 2 and Reynolds numbers of 12×10^6, if the ratio of tunnel-boundary-layer thickness to wing semispan is of the order of 1/10, correct over-all aerodynamic characteristics can be obtained by mounting the model directly to the tunnel sidewall. Local lifting pressures over inboard stations, however, can be in error approximately 5 percent at low angles of attack.

REFERENCES

1. Hatch, John E., Jr., and Hargrave, L. Keith: Effects of Reynolds Number on the Aerodynamic Characteristics of a Delta Wing at Mach Number of 2.41. NACA RM L51H06, 1951.

2. Love, Eugene S., Coletti, Donald E., and Bromm, August F., Jr.: Investigation of the Variation With Reynolds Number of the Base, Wave, and Skin-Friction Drag of a Parabolic Body of Revolution (NACA RM-10) at Mach Numbers of 1.62, 1.93, and 2.41 in Langley 9-Inch Supersonic Tunnel. NACA RM L52H21, 1952.

3. Brown, Clinton E.: Theoretical Lift and Drag of Thin Triangular Wings at Supersonic Speeds. NACA Rep. 839, 1946. (Supersedes NACA TN 1183.)

4. Wilson, R. E., Young, E. C., and Thompson, M. J.: 2nd Interim Report on Experimentally Determined Turbulent Boundary-Layer Characteristics at Supersonic Speeds. CM 501 (ut/DRL 196), Contract NOrd-9195, Bur. Ord., Univ. Texas, Defense Res. Lab. The Johns Hopkins Univ. Appl. Phys. Lab., Jan. 25, 1949.

5. Love, Eugene S., and Grigsby, Carl E.: A New Shadowgraph Technique for the Observation of Conical Flow Phenomena in Supersonic Flow and Preliminary Results Obtained for a Triangular Wing. NACA TN 2950, 1953.

TABLE I

MEASURED LOCAL FLOW ANGLES

[All angles in degrees]

$M = 1.93, \quad R = 1.3 \times 10^6$

Vane no. \ α	0°	2°	4°	6°	8°	10°
1	0.1	0.5	0.6	1.0	0.9	1.1
2	-.4	.5	1.5	2.6	3.5	4.9
3	-1.0	-.2	1.7	4.0	5.9	8.5
4	1.3	1.9	2.8	3.0	3.0	4.0
5	1.0	2.0	3.2	4.3	5.3	7.8
6	.9	2.7	4.4	7.3	10.8	13.5
7	1.0	.9	1.4	1.6	1.6	1.1
8	.5	1.1	1.6	2.1	2.2	1.8
9	1.1	1.4	1.7	2.5	2.9	3.8
10	1.1	2.2	4.1	4.0	6.6	13.2
11	1.6	3.0	5.5	6.7	11.2	16.6
12	1.6	3.5	5.8	9.7	13.5	16.4
13	1.5	3.5	6.0	10.1	13.9	16.6
14	-.5	.1	.5	.8	.3	-.2
15	1.0	2.5	3.6	4.5	9.0	14.0
16	2.1	5.0	8.3	13.1	15.8	18.3

$M = 1.62, \quad R = 1.4 \times 10^6$

Vane no. \ α	0°	2°	4°	6°	8°	10°
1	0.8	1.2	1.8	2.1	2.6	3.1
2	.4	1.2	2.1	3.1	3.9	4.9
3	-.8	.6	2.0	4.3	5.7	8.5
4	1.7	2.4	2.5	3.0	4.1	3.6
5	2.0	3.0	4.0	4.7	5.2	7.5
6	.9	2.9	5.2	7.9	11.7	15.6
7	.4	.5	.9	1.5	1.9	.4
8	1.6	2.3	2.5	2.9	2.7	3.0
9	1.6	2.0	3.0	3.4	3.0	2.3
10	2.0	2.9	3.7	4.8	6.5	9.9
11	1.6	2.8	3.8	5.0	7.6	14.8
12	1.2	2.6	5.2	5.8	11.3	18.7
13	1.7	3.8	7.2	10.1	16.1	20.6
14	-.1	0	.7	1.1	2.0	.8
15	.8	1.2	2.3	2.7	1.7	7.7
16	2.6	5.1	6.9	11.1	20.3	10.2

TABLE II.- EXPERIMENTAL PRESSURE COEFFICIENTS

$M = 1.90$

$R = 18.4 \times 10^6$																		
Station		$\alpha = 0^\circ$	$\alpha = 2^\circ$		$\alpha = 4^\circ$		$\alpha = 6^\circ$		$\alpha = 8^\circ$		$\alpha = 10^\circ$		$\alpha = 12^\circ$		$\alpha = 14^\circ$		$\alpha = 16^\circ$	
$\frac{y}{b/2}$	Percent c	C_p	C_{p_u}	C_{p_l}	C_{p_u}	C_{p_l}	C_{p_u}	C_{p_l}	C_{p_u}	C_{p_l}	C_{p_u}	C_{p_l}	C_{p_u}	C_{p_l}	C_{p_u}	C_{p_l}	C_{p_u}	C_{p_l}
0.111	0	0.218	0.206	0.215	0.176	0.197	0.145	0.164	0.109	0.127	0.079	0.082	0.058	0.034	0.043	-.020	0.030	-.057
	3.8	.044	.006	.084	-.037	.120	-.085	.155	-.121	.193	-.147	.234	-.244	.261	-.299	.324	-.303	.360
	7.3	.025	-.011	.063	-.047	.098	-.079	.134	-.111	.173	-.150	.210	-.186	.252	-.236	.299	-.279	.346
	10.6	.005	-.023	.038	-.051	.071	-.075	.106	-.103	.143	-.129	.179	-.156	.221	-.233	.267	-.282	.311
	14.2	-.003	-.026	.026	-.051	.057	-.073	.091	-.096	.131	-.119	.168	-.140	.209	-.190	.251	-.282	.295
	17.5	-.006	-.028	.024	-.050	.053	-.072	.083	-.092	.118	-.115	.150	-.131	.191	-.147	.234	-.276	.275
	21.2	-.011	-.032	.016	-.053	.043	-.072	.071	-.090	.104	-.110	.134	-.125	.173	-.123	.214	-.193	.254
	24.7	-.007	-.028	.020	-.048	.046	-.065	.075	-.087	.108	-.104	.138	-.118	.176	-.120	.216	-.145	.256
	28.2	-.007	-.027	.020	-.047	.046	-.064	.074	-.084	.107	-.103	.139	-.117	.176	-.123	.217	-.136	.257
	31.7	-.009	-.028	.016	-.048	.043	-.065	.070	-.085	.103	-.102	.133	-.118	.170	-.124	.210	-.136	.250
	38.2	-.016	-.036	.008	-.056	.033	-.072	.061	-.090	.103	-.107	.123	-.123	.159	-.129	.198	-.148	.237
	43.7	-.022	-.041	.002	-.061	.027	-.073	.056	-.092	.086	-.115	.115	-.134	.152	-.140	.190	-.153	.230
	49.2	-.035	-.051	-.010	-.066	.026	-.078	.052	-.095	.073	-.114	.101	-.131	.138	-.144	.177	-.158	.215
	55.0	-.028	-.047	-.005	-.066	.020	-.082	.046	-.098	.076	-.113	.105	-.130	.140	-.143	.180	-.159	.219
	60.7	-.031	-.049	-.007	-.069	.017	-.083	.045	-.099	.074	-.115	.105	-.132	.138	-.147	.177	-.163	.220
	66.2	-.032	-.050	-.008	-.069	.016	-.082	.045	-.099	.075	-.115	.104	-.132	.141	-.149	.180	-.161	.215
	71.7	-.032	-.051	-.008	-.069	.016	-.083	.043	-.099	.072	-.115	.103	-.132	.138	-.149	.177	-.161	.217
	77.5	-.034	-.052	-.009	-.070	.014	-.084	.042	-.101	.072	-.116	.101	-.132	.137	-.149	.175	-.165	.215
	83.2	-.037	-.055	-.014	-.073	.010	-.087	.035	-.104	.065	-.118	.094	-.134	.130	-.150	.168	-.166	.207
	88.7	-.040	-.055	-.020	-.071	.003	-.084	.027	-.101	.056	-.115	.081	-.130	.116	-.148	.152	-.163	.191
	94.0	-.064	-.077	-.048	-.092	-.029	-.103	-.007	-.118	.019	-.130	.062	-.145	.073	-.161	.107	-.174	.142
0.333	0	.171	.133	.187	.068	.171	0	.142	-.064	.101	-.105	.066	-.138	.034	-.165	0	-.197	-.032
	4.8	.009	-.019	.064	-.182	.111	-.187	.152	-.250	.193	-.298	.228	-.333	.264	-.335	.298	-.331	.333
	9.2	-.025	-.070	.023	-.127	.066	-.210	.107	-.271	.149	-.313	.187	-.343	.228	-.323	.269	-.324	.312
	14.2	-.033	-.070	.008	-.114	.046	-.164	.086	-.264	.127	-.293	.178	-.291	.208	-.313	.252	-.319	.298
	18.7	-.035	-.069	.002	-.108	.037	-.148	.076	-.201	.116	-.249	.157	-.283	.198	-.315	.242	-.323	.288
	23.2	-.037	-.067	-.003	-.100	.031	-.132	.066	-.189	.105	-.256	.143	-.289	.184	-.318	.227	-.330	.272
	28.2	-.036	-.063	-.004	-.093	.027	-.121	.062	-.170	.099	-.265	.135	-.297	.174	-.323	.216	-.334	.261
	32.7	-.037	-.062	-.006	-.090	.024	-.115	.057	-.166	.094	-.261	.130	-.305	.168	-.329	.209	-.332	.257
	40.2	-.048	-.070	-.021	-.096	.008	-.118	.038	-.133	.073	-.231	.109	-.314	.147	-.328	.197	-.342	.230
	47.5	-.047	-.066	-.023	-.087	.003	-.106	.034	-.117	.068	-.103	.101	-.296	.135	-.343	.182	-.360	.224
	55.0	-.047	-.067	-.021	-.092	.005	-.113	.035	-.127	.067	-.129	.098	-.186	.133	-.318	.172	-.351	.213
	62.7	-.054	-.072	-.030	-.094	-.005	-.112	.022	-.126	.053	-.136	.085	-.147	.118	-.258	.155	-.331	.200
	70.2	-.048	-.066	-.024	-.090	0	-.108	.028	-.121	.061	-.132	.094	-.138	.130	-.198	.158	-.301	.208
	77.5	-.057	-.073	-.034	-.095	-.009	-.112	.018	-.128	.049	-.143	.080	-.153	.115	-.189	.150	-.280	.192
	85.0	-.060	-.077	-.037	-.097	-.014	-.114	.012	-.129	.042	-.145	.073	-.156	.103	-.180	.136	-.254	.188
	92.5	-.065	-.076	-.043	-.100	-.022	-.117	.005	-.131	.033	-.146	.063	-.157	.096	-.188	.132	-.236	.182
0.555	0	.163	.142	.150	.083	.096	.019	.026	-.036	-.041	-.082	-.068	-.119	-.130	-.149	-.164	-.173	-.192
	7.5	-.084	-.093	.044	-.162	.098	-.222	.144	-.290	.187	-.330	.227	-.341	.258	-.384	.290	-.326	.320
	14.2	-.057	-.121	.002	-.205	.051	-.259	.112	-.307	.169	-.339	.193	-.324	.227	-.318	.262	-.320	.299
	21.2	-.060	-.115	-.019	-.197	.023	-.272	.069	-.316	.119	-.326	.157	-.319	.193	-.318	.240	-.323	.281
	28.7	-.066	-.112	-.020	-.157	.019	-.259	.058	-.270	.100	-.290	.135	-.318	.187	-.321	.220	-.326	.262
	35.2	-.067	-.102	-.027	-.145	.005	-.208	.046	-.249	.087	-.288	.125	-.318	.164	-.325	.205	-.328	.251
	42.2	-.068	-.097	-.032	-.136	.006	-.202	.044	-.254	.061	-.288	.118	-.321	.154	-.330	.198	-.333	.243
	55.0	-.069	-.098	-.037	-.131	-.006	-.183	.029	-.267	.066	-.300	.099	-.331	.136	-.335	.177	-.334	.221
	66.3	-.067	-.091	-.037	-.118	-.007	-.150	.025	-.265	.060	-.308	.093	-.333	.127	-.336	.166	-.338	.211
	77.5	-.077	-.099	-.048	-.123	-.022	-.141	.008	-.255	.041	-.318	.073	-.338	.109	-.339	.147	-.347	.188
	88.7	-.085	-.104	-.061	-.124	-.035	-.135	-.005	-.210	.028	-.316	.059	-.337	.092	-.347	.129	-.356	.168
0.777	0	.118	.087	.071	.006	-.006	-.096	-.081	-.167	-.113	-.214	-.156	-.259	-.184	-.285	-.210	-.301	-.226
	11.2	-.092	-.177	-.015	-.242	.043	-.287	.096	-.337	.139	-.357	.175	-.347	.209	-.340	.237	-.326	.265
	22.4	-.114	-.190	-.041	-.267	-.016	-.309	.054	-.348	.107	-.355	.143	-.330	.185	-.325	.225	-.324	.258
	33.6	-.117	-.154	-.056	-.272	-.005	-.314	.041	-.348	.083	-.344	.122	-.326	.163	-.324	.202	-.325	.240
	44.8	-.123	-.188	-.063	-.272	-.017	-.315	.082	-.348	.065	-.336	.098	-.327	.143	-.327	.183	-.330	.222
	56.0	-.115	-.170	-.064	-.265	-.022	-.314	.017	-.292	.057	-.329	.091	-.328	.132	-.328	.182	-.332	.212
	67.2	-.104	-.152	-.059	-.239	-.017	-.267	.021	-.285	.057	-.324	.091	-.329	.131	-.331	.183	-.334	.213
	78.4																	

CONFIDENTIAL

[redacted]

[redacted]

TABLE II.- EXPERIMENTAL PRESSURE COEFFICIENTS - Continued

$M = 1.90$

$R = 12.6 \times 10^6$

Station		$\alpha = 0^\circ$	$\alpha = 2^\circ$		$\alpha = 4^\circ$		$\alpha = 6^\circ$		$\alpha = 8^\circ$		$\alpha = 10^\circ$		$\alpha = 12^\circ$		$\alpha = 14^\circ$		$\alpha = 16^\circ$	
$\frac{y}{b/2}$	Percent c	C_p	C_{p_u}	C_{p_l}	C_{p_u}	C_{p_l}	C_{p_u}	C_{p_l}	C_{p_u}	C_{p_l}	C_{p_u}	C_{p_l}	C_{p_u}	C_{p_l}	C_{p_u}	C_{p_l}	C_{p_u}	C_{p_l}
0.111	0	0.215	0.204	0.216	0.177	0.196	0.135	0.164	0.115	0.122	0.078	0.072	0.055	0.030	0.043	-.021	0.030	-.061
	3.8	.042	.006	.085	-.038	.118	-.087	.153	-.122	.194	-.146	.231	-.237	.279	-.283	.320	-.301	.361
	7.3	.025	-.008	.063	-.045	.096	-.082	.131	-.108	.171	-.148	.203	-.182	.250	-.247	.294	-.284	.340
	10.6	.003	-.024	.037	-.052	.068	-.082	.108	-.101	.141	-.128	.173	-.153	.217	-.223	.260	-.282	.306
	14.2	-.004	-.029	.025	-.054	.055	-.079	.089	-.096	.128	-.119	.162	-.139	.205	-.190	.246	-.279	.291
	17.5	-.007	-.030	.023	-.054	.051	-.078	.082	-.092	.116	-.114	.146	-.133	.188	-.154	.228	-.270	.270
	21.2	-.012	-.032	.017	-.054	.043	-.077	.071	-.090	.104	-.111	.132	-.126	.173	-.126	.211	-.199	.252
	24.7	-.007	-.027	.020	-.049	.046	-.073	.076	-.085	.108	-.104	.136	-.120	.177	-.118	.214	-.150	.253
	28.2	-.009	-.029	.020	-.050	.045	-.072	.072	-.085	.106	-.103	.135	-.118	.174	-.123	.213	-.140	.253
	31.7	-.010	-.030	.017	-.050	.041	-.072	.069	-.085	.102	-.103	.131	-.119	.170	-.124	.206	-.137	.247
	38.2	-.018	-.037	.009	-.058	.032	-.079	.060	-.091	.092	-.108	.120	-.124	.158	-.133	.195	-.148	.234
	43.7	-.020	-.042	.003	-.062	.026	-.082	.054	-.096	.086	-.113	.113	-.128	.151	-.142	.188	-.156	.227
	49.2	-.021	-.043	.003	-.065	.026	-.086	.052	-.097	.083	-.114	.111	-.131	.151	-.143	.187	-.159	.226
	55.0	-.028	-.047	-.003	-.066	.020	-.087	.046	-.096	.077	-.113	.103	-.127	.142	-.144	.179	-.159	.217
	60.7	-.029	-.048	-.005	-.068	.016	-.088	.043	-.098	.075	-.115	.103	-.131	.139	-.146	.180	-.162	.220
	66.2	-.031	-.050	-.006	-.068	.018	-.089	.046	-.098	.077	-.114	.105	-.132	.142	-.148	.181	-.160	.220
	71.7	-.032	-.051	-.007	-.068	.015	-.090	.040	-.098	.074	-.113	.102	-.133	.139	-.143	.177	-.163	.216
	77.5	-.033	-.051	-.009	-.070	.014	-.091	.041	-.099	.072	-.113	.099	-.133	.137	-.149	.175	-.164	.214
	83.2	-.037	-.054	-.013	-.073	.009	-.093	.037	-.101	.068	-.118	.093	-.135	.132	-.149	.168	-.166	.206
	88.7	-.040	-.056	-.019	-.072	.002	-.093	.028	-.099	.057	-.115	.082	-.132	.118	-.147	.154	-.164	.191
	94.0	-.067	-.077	-.047	-.091	-.028	-.109	-.005	-.117	.022	-.130	.045	-.145	.078	-.159	.113	-.175	.147
0.333	0	.173	.132	.186	.069	.171	0	.140	-.068	.098	-.108	.064	-.146	.033	-.173	-.002	-.203	-.035
	4.8	.009	-.051	.064	-.123	.113	-.186	.156	-.256	.196	-.298	.232	-.326	.267	-.324	.304	-.321	.334
	9.2	-.027	-.075	.021	-.131	.066	-.209	.107	-.274	.150	-.312	.189	-.328	.229	-.322	.274	-.319	.311
	14.2	-.036	-.075	.007	-.117	.049	-.163	.087	-.267	.129	-.313	.169	-.309	.210	-.315	.257	-.318	.298
	18.7	-.038	-.074	0	-.111	.037	-.143	.073	-.200	.114	-.244	.153	-.294	.194	-.315	.241	-.325	.282
	23.2	-.040	-.071	-.006	-.103	.029	-.131	.066	-.185	.103	-.243	.142	-.293	.180	-.318	.225	-.328	.265
	28.2	-.037	-.066	-.004	-.095	.029	-.124	.062	-.168	.100	-.250	.138	-.297	.176	-.322	.219	-.332	.261
	33.7	-.042	-.068	-.012	-.094	.018	-.120	.053	-.152	.086	-.247	.130	-.297	.171	-.327	.216	-.335	.258
	40.2	-.048	-.072	-.020	-.097	.010	-.117	.041	-.138	.076	-.219	.110	-.299	.146	-.329	.188	-.345	.226
	47.5	-.052	-.073	-.026	-.094	.002	-.109	.034	-.126	.069	-.133	.100	-.284	.135	-.341	.183	-.359	.219
	55.0	-.048	-.071	-.023	-.094	.006	-.112	.036	-.129	.066	-.129	.100	-.197	.135	-.320	.178	-.348	.212
	62.7	-.052	-.074	-.027	-.095	-.003	-.111	.026	-.127	.057	-.135	.090	-.150	.122	-.272	.163	-.325	.201
	70.2	-.048	-.069	-.024	-.091	.002	-.109	.030	-.124	.064	-.132	.097	-.146	.133	-.218	.173	-.298	.211
	77.5	-.055	-.075	-.032	-.095	-.006	-.111	.023	-.128	.053	-.140	.086	-.156	.120	-.197	.159	-.276	.195
	85.0	-.058	-.078	-.036	-.098	-.012	-.114	.015	-.130	.046	-.143	.076	-.158	.107	-.185	.146	-.250	.180
	92.5	-.063	-.084	-.043	-.103	-.019	-.117	.008	-.132	.039	-.144	.069	-.159	.102	-.183	.140	-.223	.176
0.555	0	.167	.146	.146	.083	.094	.011	.024	-.044	-.043	-.085	-.089	-.128	-.131	-.155	-.166	-.181	-.197
	7.5	-.085	-.097	.044	-.164	.100	-.223	.145	-.298	.189	-.325	.227	-.328	.257	-.324	.292	-.324	.320
	14.2	-.058	-.123	.002	-.209	.062	-.259	.120	-.311	.158	-.335	.195	-.328	.228	-.318	.267	-.319	.301
	21.2	-.066	-.112	-.025	-.200	.023	-.272	.072	-.321	.117	-.338	.157	-.323	.196	-.320	.246	-.324	.278
	28.7	-.061	-.112	-.019	-.158	.021	-.252	.063	-.296	.102	-.302	.136	-.317	.179	-.321	.224	-.325	.262
	35.2	-.066	-.101	-.030	-.144	.007	-.207	.048	-.246	.089	-.288	.127	-.313	.166	-.324	.212	-.327	.252
	42.2	-.069	-.101	-.032	-.140	.006	-.200	.040	-.248	.081	-.286	.120	-.317	.156	-.327	.204	-.332	.242
	55.0	-.069	-.098	-.037	-.131	-.003	-.183	.030	-.262	.065	-.293	.102	-.322	.138	-.332	.180	-.335	.216
	66.3	-.066	-.094	-.037	-.121	-.004	-.157	.027	-.262	.062	-.294	.096	-.323	.127	-.336	.172	-.341	.212
	77.5	-.074	-.099	-.046	-.124	-.018	-.146	.010	-.253	.044	-.305	.079	-.331	.113	-.340	.155	-.352	.191
	88.7	-.084	-.106	-.060	-.126	-.090	-.140	-.003	-.218	.041	-.306	.063	-.331	.095	-.347	.136	-.356	.172
0.777	0	.164	-.074	.075	-.002	-.003	-.099	-.064	-.158	-.114	-.210	-.154	-.252	-.185	-.200	-.209	-.298	-.227
	11.2	-.090	-.172	-.013	-.242	.045	-.283	.099	-.326	.142	-.348	.172	-.347	.210	-.344	.239	-.329	.265
	22.4	-.111	-.188	-.039	-.269	.016	-.305	.065	-.339	.108	-.347	.143	-.347	.188	-.320	.224	-.322	.257
	33.6	-.119	-.161	-.053	-.273	-.004	-.306	.040	-.340	.085	-.345	.119	-.329	.164	-.318	.202	-.325	.240
	44.8	-.120	-.181	-.063	-.273	-.019	-.308	.023	-.339	.065	-.337	.100	-.324	.142	-.321	.181	-.328	.220
	56.0	-.113	-.168	-.063	-.269	-.021	-.311	.019	-.335	.060	-.333	.091	-.325	.136	-.325	.174	-.331	.214
	67.2	-.102	-.149	-.055	-.221	-.016	-.273	.023	-.321	.061	-.326	.091	-.325	.134	-.327	.174	-.332	.215
	78.4																	

TABLE II. - EXPERIMENTAL PRESSURE COEFFICIENTS - Continued

$M = 1.93$

$R = 7.2 \times 10^6$											
Station		$\alpha = 0^\circ$	$\alpha = 2^\circ$		$\alpha = 4^\circ$		$\alpha = 6^\circ$		$\alpha = 8^\circ$		$\alpha = 10^\circ$	
$\frac{y}{b/2}$	Percent c	C_p	C_{p_u}	C_{p_l}	C_{p_u}	C_{p_l}	C_{p_u}	C_{p_l}	C_{p_u}	C_{p_l}	C_{p_u}	C_{p_l}
0.111	0	0.193	0.182	0.194	0.159	0.175	0.129	0.151	0.094	0.069	0.068	0.075
	3.8	.054	.020	.095	-.019	.133	-.057	.167	-.103	.195	-.155	.224
	7.3	.017	.008	.070	-.025	.104	-.053	.137	-.089	.178	-.117	.219
	10.6	.010	-.015	.040	-.038	.072	-.062	.105	-.090	.146	-.113	.184
	14.2	.006	-.020	.034	-.041	.064	-.062	.100	-.086	.138	-.105	.176
	17.5	.004	-.019	.029	-.040	.058	-.059	.089	-.082	.124	-.102	.159
	21.2	-.002	-.023	.022	-.043	.048	-.063	.077	-.083	.108	-.101	.143
	24.7	-.001	-.024	.024	-.043	.049	-.061	.077	-.081	.108	-.100	.142
	28.2	-.004	-.025	.020	-.044	.049	-.062	.072	-.082	.104	-.100	.138
	31.7	-.007	-.027	.018	-.047	.040	-.064	.068	-.086	.100	-.101	.138
	38.2	-.017	-.036	.018	-.057	.040	-.082	.056	-.091	.088	-.108	.135
	43.7	-.023	-.043	.002	-.063	.021	-.076	.047	-.097	.077	-.113	.109
	49.2	-.026	-.045	.003	-.065	.019	-.080	.044	-.097	.074	-.113	.106
	55.0	-.036	-.055	-.014	-.075	.006	-.089	.031	-.105	.059	-.119	.090
	60.7	-.028	-.047	-.005	-.068	.017	-.082	.043	-.098	.072	-.113	.104
	66.2	-.033	-.053	-.011	-.072	.011	-.087	.037	-.102	.066	-.116	.098
	71.7	-.037	-.055	-.016	-.072	.006	-.087	.032	-.103	.064	-.116	.096
	77.5	-.040	-.060	-.017	-.077	.004	-.092	.030	-.107	.059	-.121	.091
	83.2	-.049	-.067	-.028	-.084	-.007	-.098	.018	-.113	.043	-.126	.075
	88.7	-.046	-.064	-.025	-.082	-.004	-.096	.022	-.111	.049	-.125	.080
	94.0	-.073	-.085	-.054	-.099	-.034	-.101	-.011	-.125	.015	-.138	.044
0.333	0	.171	.134	.184	.072	.168	.007	.132	-.064	.088	-.098	.051
	4.8	.017	-.046	.072	-.120	.118	-.172	.157	-.239	.197	-.285	.235
	9.2	-.018	-.062	.026	-.124	.074	-.198	.113	-.258	.157	-.300	.198
	14.2	-.033	-.069	.010	-.114	.048	-.163	.086	-.258	.128	-.293	.168
	18.7	-.033	-.068	.005	-.109	.041	-.141	.076	-.197	.115	-.262	.155
	23.2	-.032	-.063	.003	-.098	.036	-.128	.069	-.172	.106	-.236	.146
	28.2	-.042	-.069	-.009	-.100	.022	-.126	.053	-.162	.089	-.234	.126
	32.7	-.043	-.067	-.013	-.096	.017	-.120	.046	-.149	.081	-.225	.117
	40.2	-.052	-.077	-.026	-.101	.001	-.122	.029	-.143	.062	-.200	.097
	47.5	-.053	-.076	-.028	-.099	-.002	-.119	.028	-.136	.060	-.158	.093
	55.0	-.056	-.075	-.031	-.096	-.007	-.128	.021	-.129	.053	-.131	.087
	62.7	-.055	-.076	-.031	-.097	-.007	-.114	.019	-.131	.049	-.135	.082
	70.2	-.056	-.075	-.032	-.096	-.009	-.118	.017	-.129	.048	-.135	.080
	77.5	-.056	-.075	-.032	-.097	-.008	-.126	.017	-.128	.048	-.136	.079
	85.0	-.063	-.081	-.036	-.100	-.019	-.117	.007	-.133	.039	-.142	.069
	92.5	-.069	-.091	-.049	-.109	-.028	-.124	-.006	-.139	.023	-.150	.050
0.555	0	.166	.148	.150	.087	.097	.023	.031	-.032	-.032	-.070	-.082
	7.5	-.023	-.093	.045	-.165	.096	-.220	.137	-.284	.181	-.318	.216
	14.2	-.055	-.118	.003	-.203	.049	-.255	.094	-.300	.137	-.329	.179
	21.2	-.073	-.120	-.020	-.200	.020	-.267	.058	-.309	.099	-.319	.142
	28.7	-.074	-.117	-.029	-.167	-.003	-.265	.046	-.310	.086	-.316	.125
	35.2	-.076	-.112	-.038	-.153	-.002	-.211	.033	-.282	.072	-.302	.111
	42.2	-.075	-.107	-.038	-.144	-.006	-.193	.030	-.247	.066	-.292	.104
	55.0	-.080	-.106	-.047	-.138	-.020	-.175	.017	-.238	.051	-.287	.084
	66.3	-.071	-.096	-.040	-.124	-.010	-.155	.020	-.234	.054	-.287	.089
	77.5	-.073	-.098	-.046	-.123	-.033	-.147	.010	-.223	.043	-.289	.073
	88.7	-.083	-.105	-.059	-.128	-.035	-.147	-.004	-.209	.025	-.292	.055
0.777	0	.119	.098	.084	.017	.020	-.063	-.009	-.131	-.078	-.176	-.116
	11.2	-.078	-.161	-.002	-.229	.053	-.273	.102	-.320	.146	-.342	.183
	22.4	-.107	-.182	-.039	-.258	.017	-.295	.068	-.330	.114	-.329	.156
	33.6	-.113	-.180	-.054	-.265	-.006	-.301	.038	-.333	.082	-.330	.121
	44.8	-.118	-.181	-.067	-.266	-.023	-.305	.022	-.335	.064	-.330	.103
	56.0	-.110	-.163	-.063	-.257	-.022	-.303	.019	-.334	.058	-.330	.096
	67.2	-.106	-.150	-.063	-.228	-.023	-.300	.014	-.332	.055	-.327	.088
	78.4	-.105	-.146	-.066	-.199	-.033	-.284	.007	-.318	.033	-.324	.078

[redacted]

TABLE II. - EXPERIMENTAL PRESSURE COEFFICIENTS - Concluded

M = 1.93

R = 2.2 x 10^6												
Station		$\alpha = 0^\circ$	$\alpha = 2^\circ$		$\alpha = 4^\circ$		$\alpha = 6^\circ$		$\alpha = 8^\circ$		$\alpha = 10^\circ$	
$\frac{y}{b/2}$	Percent c	C_p	C_{p_u}	C_{p_l}	C_{p_u}	C_{p_l}	C_{p_u}	C_{p_l}	C_{p_u}	C_{p_l}	C_{p_u}	C_{p_l}
0.111	0	0.196	0.187	0.195	0.155	0.177	0.123	0.152	0.088	0.117	0.063	0.078
	3.8	.056	.021	.089	-.021	.125	-.056	.157	-.099	.190	-.143	.224
	7.3	.029	.001	.060	-.029	.093	-.058	.127	-.097	.165	-.141	.204
	10.6	.010	-.014	.037	-.040	.073	-.065	.107	-.099	.144	-.120	.184
	14.2	.004	-.018	.031	-.042	.062	-.067	.096	-.092	.132	-.095	.168
	17.5	.003	-.020	.029	-.043	.058	-.068	.087	-.079	.121	-.091	.157
	21.2	0	-.022	.025	-.045	.051	-.064	.078	-.074	.110	-.091	.144
	24.7	.001	-.021	.025	-.043	.051	-.056	.078	-.073	.110	-.089	.143
	28.2	-.001	-.021	.021	-.042	.047	-.056	.073	-.074	.105	-.090	.138
	31.7	-.002	-.022	.020	-.042	.045	-.057	.071	-.076	.102	-.092	.135
	38.2	-.012	-.033	.008	-.051	.033	-.066	.059	-.084	.089	-.099	.122
	43.7	-.017	-.037	.002	-.056	.028	-.070	.052	-.088	.082	-.104	.114
	49.2	-.020	-.038	0	-.057	.025	-.073	.049	-.091	.078	-.107	.111
	55.0	-.026	-.046	-.007	-.063	.016	-.078	.041	-.095	.069	-.110	.102
	60.7	-.022	-.043	-.004	-.061	.020	-.075	.045	-.093	.074	-.108	.107
	66.2	-.026	-.045	-.006	-.064	.016	-.078	.041	-.097	.070	-.111	.103
	71.7	-.032	-.052	-.011	-.069	.011	-.084	.035	-.101	.064	-.115	.096
	77.5	-.034	-.052	-.013	-.070	.009	-.086	.034	-.102	.062	-.118	.094
	83.2	-.038	-.059	-.021	-.075	.002	-.091	.025	-.107	.053	-.122	.085
	88.7	-.039	-.058	-.019	-.075	.004	-.092	.026	-.108	.055	-.122	.086
	94.0	-.064	-.078	-.048	-.092	-.027	-.104	-.005	-.120	.021	-.133	.051
0.333	0	.159	.125	.166	.065	.152	.001	.121	-.068	.075	-.105	.043
	4.8	.014	-.041	.064	-.106	.108	-.166	.148	-.205	.167	-.247	.224
	9.2	-.014	-.061	.027	-.110	.066	-.150	.109	-.198	.151	-.243	.192
	14.2	-.029	-.067	.010	-.105	.046	-.155	.084	-.210	.125	-.251	.167
	18.7	-.030	-.064	.005	-.100	.038	-.170	.074	-.221	.113	-.254	.154
	23.2	-.032	-.064	-.002	-.106	.029	-.166	.064	-.219	.102	-.255	.136
	28.2	-.036	-.065	-.007	-.105	.022	-.151	.056	-.206	.091	-.252	.130
	32.7	-.039	-.066	-.010	-.102	.016	-.110	.048	-.175	.085	-.240	.120
	40.2	-.047	-.071	-.020	-.091	.009	-.103	.038	-.136	.068	-.218	.102
	47.5	-.045	-.072	-.018	-.085	.005	-.105	.034	-.125	.065	-.181	.100
	55.0	-.045	-.071	-.021	-.086	0	-.106	.028	-.123	.060	-.147	.093
	62.7	-.047	-.066	-.023	-.087	-.002	-.104	.024	-.121	.056	-.130	.088
	70.2	-.049	-.066	-.025	-.087	-.004	-.104	.018	-.122	.052	-.130	.084
	77.5	-.049	-.067	-.025	-.087	-.006	-.105	.021	-.121	.050	-.130	.082
	85.0	-.056	-.073	-.034	-.092	-.012	-.109	.017	-.125	.043	-.135	.073
	92.5	-.060	-.077	-.037	-.098	-.013	-.113	.007	-.130	.033	-.140	.064
0.555	0	.161	.141	.140	.085	.087	.018	.026	-.038	.051	-.077	-.086
	7.5	-.021	-.089	.041	-.159	.088	-.215	.132	-.271	.172	-.279	.212
	14.2	-.054	-.115	-.001	-.171	.044	-.210	.089	-.258	.134	-.278	.179
	21.2	-.069	-.120	-.025	-.165	.016	-.212	.061	-.260	.102	-.280	.145
	28.7	-.070	-.111	-.028	-.171	.008	-.220	.056	-.266	.088	-.285	.128
	35.2	-.070	-.107	-.032	-.172	.002	-.232	.038	-.271	.076	-.287	.116
	42.2	-.073	-.112	-.038	-.172	-.006	-.231	.030	-.273	.067	-.290	.112
	55.0	-.075	-.108	-.041	-.138	-.015	-.206	.018	-.271	.056	-.288	.091
	66.3	-.070	-.100	-.034	-.104	-.003	-.149	.026	-.248	.058	-.282	.091
	77.5	-.067	-.092	-.038	-.109	-.015	-.128	.013	-.229	.044	-.283	.083
	88.7	-.075	-.096	-.052	-.117	-.026	-.132	0	-.208	.027	-.285	.060
0.777	0	.126	.095	.094	.019	.029	-.063	-.027	-.134	-.079	-.180	-.118
	11.2	-.078	.159	-.006	-.226	.053	-.271	.100	-.290	.144	-.297	.185
	22.4	-.107	-.178	-.041	-.237	.016	-.260	.063	-.284	.110	-.297	.154
	33.6	-.114	-.171	-.056	-.233	-.005	-.262	.038	-.236	.083	-.299	.124
	44.8	-.116	-.168	-.069	-.239	-.021	-.267	.019	-.288	.061	-.302	.101
	56.0	-.110	-.168	-.067	-.242	-.025	-.272	.014	-.289	.053	-.304	.093
	67.2	-.104	-.166	-.063	-.239	-.024	-.279	.012	-.291	.053	-.305	.098
	78.4	-.106	-.164	-.069	-.238	-.032	-.275	.012	-.291	.043	-.306	.082

TABLE III. - EXPERIMENTAL PRESSURE COEFFICIENTS

M = 1.62

$R = 7.2 \times 10^6$												
Station		$\alpha = 0^\circ$	$\alpha = 2^\circ$		$\alpha = 4^\circ$		$\alpha = 6^\circ$		$\alpha = 8^\circ$		$\alpha = 10^\circ$	
$\frac{y}{b/2}$	Percent c	C_p	C_{p_u}	C_{p_l}	C_{p_u}	C_{p_l}	C_{p_u}	C_{p_l}	C_{p_u}	C_{p_l}	C_{p_u}	C_{p_l}
0.111	0	0.210	0.193	0.201	0.163	0.181	0.122	0.147	0.068	0.098	0.023	0.037
	3.8	.048	.009	.094	-.029	.134	-.068	.168	-.113	.203	-.154	.239
	7.3	.052	.018	.086	-.017	.124	-.051	.163	-.086	.205	-.122	.251
	10.6	.030	0	.063	-.031	.096	-.060	.131	-.090	.168	-.117	.210
	14.2	.025	-.001	.056	-.031	.088	-.060	.121	-.086	.158	-.110	.200
	17.5	.017	-.010	.048	-.037	.079	-.062	.113	-.086	.149	-.109	.187
	21.2	.008	-.016	.038	-.041	.067	-.064	.099	-.087	.135	-.108	.174
	24.7	.008	-.015	.037	-.040	.066	-.061	.098	-.084	.133	-.105	.171
	28.2	.006	-.018	.033	-.041	.062	-.062	.093	-.084	.128	-.105	.166
	31.7	.003	-.021	.029	-.043	.057	-.063	.087	-.086	.120	-.107	.157
	38.2	-.009	-.031	.016	-.053	.043	-.073	.072	-.094	.106	-.114	.142
	43.7	-.014	-.036	.012	-.058	.039	-.078	.067	-.099	.100	-.118	.136
	49.2	-.017	-.039	.008	-.060	.035	-.079	.063	-.099	.095	-.118	.129
	55.0											
	60.7	-.021	-.042	.005	-.063	.031	-.081	.060	-.099	.093	-.116	.125
	66.2	-.029	-.050	-.004	-.071	.024	-.089	.050	-.107	.081	-.125	.117
	71.7	-.036	-.057	-.013	-.076	.013	-.093	.041	-.111	.072	-.128	.106
	77.5	-.043	-.063	-.021	-.082	.004	-.099	.031	-.117	.063	-.134	.097
	83.2	-.061	-.080	-.040	-.098	-.017	-.114	.010	-.131	.040	-.147	.073
	88.7	-.056	-.075	-.033	-.093	-.008	-.110	.020	-.128	.053	-.143	.092
	94.0	-.089	-.103	-.072	-.118	-.052	-.133	-.024	-.149	.008	-.163	.052
0.333	0	.184	.135	.192	.041	.157	-.067	.100	-.152	.042	-.199	-.014
	4.8	.021	-.035	.082	-.128	.131	-.249	.174	-.343	.214	-.418	.252
	9.2	-.012	-.065	.041	-.131	.089	-.188	.130	-.328	.175	-.399	.219
	14.2	-.024	-.069	.021	-.122	.065	-.165	.107	-.328	.150	-.362	.193
	18.7	-.021	-.061	.020	-.103	.285	-.141	.099	-.223	.140	-.332	.183
	23.2	-.020	-.056	.017	-.093	.054	-.126	.091	-.181	.130	-.277	.172
	28.2	-.033	-.064	.001	-.097	.036	-.127	.070	-.158	.108	-.191	.149
	32.7	-.035	-.064	-.003	-.094	.030	-.121	.065	-.156	.101	-.130	.141
	40.2	-.047	-.074	-.017	-.101	.015	-.126	.050	-.148	.084	-.155	.123
	47.5	-.046	-.070	-.017	-.095	.014	-.117	.043	-.151	.076	-.148	.114
	55.0	-.048	-.071	-.021	-.096	.007	-.118	.046	-.140	.079	-.150	.116
	62.7	-.049	-.070	-.024	-.092	.004	-.113	.034	-.134	.064	-.149	.101
	70.2	-.054	-.076	-.030	-.098	-.003	-.117	.026	-.138	.055	-.152	.091
	77.5	-.060	-.080	-.037	-.101	-.010	-.119	.017	-.140	.050	-.153	.084
	85.0	-.075	-.093	-.053	-.115	-.026	-.134	.004	-.154	.033	-.167	.067
	92.5	-.088	-.108	-.063	-.127	-.040	-.144	-.008	-.162	.024	-.174	.070
0.555	0	.171	.134	.144	.040	.054	-.061	-.050	-.135	-.139	-.184	-.200
	7.5	-.014	-.105	.060	-.233	.116	-.320	.162	-.426	.202	-.435	.237
	14.2	-.048	-.116	.015	-.211	.068	-.344	.116	-.420	.160	-.426	.202
	21.2	-.063	-.117	-.012	-.183	.038	-.273	.083	-.394	.127	-.407	.168
	28.7	-.065	-.108	-.020	-.160	.023	-.215	.066	-.352	.107	-.383	.148
	35.2	-.069	-.110	-.029	-.153	.011	-.192	.051	-.342	.096	-.380	.140
	42.2	-.071	-.106	-.032	-.145	.012	-.177	.052	-.325	.089	-.387	.127
	55.0	-.079	-.105	-.055	-.137	-.009	-.167	.022	-.240	.061	-.404	.099
	66.3	-.070	-.100	-.040	-.129	-.010	-.149	.021	-.134	.057	-.381	.087
	77.5	-.086	-.113	-.057	-.139	-.029	-.159	-.005	-.158	.042	-.364	.083
	88.7	-.102	-.129	-.073	-.153	-.039	-.174	-.009	-.180	.023	-.286	.058
0.777	0	.132	.083	.065	-.057	-.046	-.177	-.125	-.264	-.191	-.323	-.242
	11.2	-.103	-.219	-.001	-.345	.065	-.419	.114	-.483	.154	-.448	.191
	22.4	-.115	-.220	-.032	-.368	.025	-.433	.073	-.467	.116	-.405	.154
	33.6	-.119	-.197	-.058	-.353	-.008	-.434	.036	-.464	.080	-.383	.122
	44.8	-.129	-.186	-.078	-.271	-.027	-.424	.014	-.453	.080	-.391	.098
	56.0	-.126	-.167	-.074	-.229	-.026	-.351	.014	-.431	.080	-.397	.101
	67.2	-.119	-.164	-.072	-.210	-.029	-.325	.015	-.425	.059	-.402	.107
	78.4	-.125	-.165	-.083	-.206	-.039	-.324	.003	-.420	.046	-.408	.085

TABLE III. - EXPERIMENTAL PRESSURE COEFFICIENTS - Concluded

M = 1.62

R = 2.4 x 10^6												
Station		α = 0°	α = 2°		α = 4°		α = 6°		α = 8°		α = 10°	
$\frac{y}{b/2}$	Percent c	C_p	C_{p_u}	C_{p_l}	C_{p_u}	C_{p_l}	C_{p_u}	C_{p_l}	C_{p_u}	C_{p_l}	C_{p_u}	C_{p_l}
0.111	0	0.201	0.187	0.190	0.156	0.172	0.116	0.137	0.068	0.091	0.020	0.036
	3.8	.048	.009	.081	-.027	.125	-.065	.160	-.114	.196	-.178	.233
	7.3	.035	.002	.066	-.033	.106	-.065	.145	-.110	.189	-.133	.232
	10.6	.019	-.011	.046	-.042	.084	-.071	.119	-.100	.156	-.116	.196
	14.2	.014	-.014	.044	-.045	.081	-.071	.114	-.089	.151	-.109	.187
	17.5	.009	-.019	.037	-.047	.071	-.068	.103	-.084	.139	-.108	.178
	21.2	.008	-.021	.032	-.047	.064	-.063	.095	-.083	.130	-.106	.168
	24.7	.008	-.020	.031	-.043	.062	-.060	.092	-.080	.126	-.104	.163
	28.2	.005	-.019	.027	-.041	.057	-.061	.086	-.080	.121	-.103	.158
	31.7	.002	-.022	.023	-.044	.053	-.062	.083	-.084	.115	-.106	.151
	38.2	-.008	-.030	.014	-.053	.040	-.071	.070	-.091	.102	-.113	.137
	43.7	-.014	-.037	.008	-.058	.035	-.077	.063	-.096	.095	-.118	.130
	49.2	-.017	-.038	.004	-.060	.032	-.078	.061	-.098	.092	-.119	.125
	55.0											
	60.7	-.020	-.042	-.001	-.062	.027	-.082	.055	-.102	.087	-.122	.121
	66.2	-.026	-.046	-.007	-.068	.021	-.086	.049	-.107	.081	-.126	.115
	71.7	-.036	-.056	-.017	-.076	.011	-.094	.039	-.113	.070	-.131	.103
	77.5	-.041	-.060	-.023	-.080	.005	-.098	.032	-.118	.064	-.137	.099
	83.2	-.051	-.069	-.032	-.089	-.005	-.106	.023	-.125	.054	-.144	.092
	88.7	-.051	-.071	-.031	-.090	-.005	-.109	.026	-.126	.062	-.143	.104
	94.0	-.081	-.095	-.068	-.111	-.044	-.128	-.014	-.146	.026	-.163	.078
0.333	0	.165	.119	.173	.032	.143	-.072	.091	-.163	.030	-.205	-.022
	4.8	.011	-.049	.071	-.133	.118	-.195	.159	-.280	.200	-.352	.240
	9.2	-.018	-.071	.034	-.129	.077	-.185	.121	-.295	.166	-.355	.211
	14.2	-.029	-.074	.016	-.116	.057	-.197	.097	-.287	.143	-.349	.189
	18.7	-.030	-.068	.012	-.119	.050	-.185	.089	-.240	.132	-.312	.174
	23.2	-.032	-.068	.005	-.116	.040	-.138	.077	-.152	.128	-.279	.164
	28.2	-.038	-.070	-.002	-.111	.031	-.107	.065	-.143	.106	-.250	.146
	32.7	-.039	-.071	-.008	-.096	.023	-.108	.059	-.139	.098	-.214	.136
	40.2	-.047	-.076	-.017	-.095	.014	-.118	.048	-.145	.083	-.171	.121
	47.5	-.046	-.075	-.018	-.091	.016	-.114	.043	-.137	.078	-.146	.114
	55.0	-.047	-.070	-.018	-.092	.015	-.113	.044	-.136	.078	-.147	.110
	62.7	-.053	-.068	-.023	-.091	.004	-.110	.032	-.135	.066	-.146	.098
	70.2	-.056	-.071	-.026	-.095	-.005	-.114	.023	-.138	.057	-.149	.089
	77.5	-.061	-.077	-.035	-.100	-.011	-.119	.017	-.141	.051	-.153	.086
	85.0	-.071	-.089	-.047	-.110	-.020	-.129	.010	-.152	.044	-.164	.083
	92.5	-.074	-.091	-.052	-.114	-.020	-.133	.014	-.155	.054	-.168	.110
0.555	0	.161	.122	.128	.035	.044	-.061	-.054	-.140	-.142	-.189	-.202
	7.5	-.026	-.113	.046	-.214	.101	-.300	.145	-.370	.189	-.379	.229
	14.2	-.059	-.122	.005	-.201	.056	-.297	.102	-.382	.151	-.386	.196
	21.2	-.070	-.122	-.018	-.203	.029	-.294	.070	-.381	.118	-.384	.164
	28.7	-.071	-.117	-.026	-.197	.016	-.279	.057	-.371	.101	-.384	.146
	35.2	-.073	-.115	-.032	-.182	.008	-.193	.051	-.340	.097	-.386	.140
	42.2	-.075	-.119	-.035	-.138	.005	-.157	.041	-.274	.080	-.390	.121
	55.0	-.081	-.115	-.047	-.126	-.020	-.152	.020	-.194	.057	-.400	.095
	66.3	-.080	-.099	-.046	-.125	-.009	-.149	.023	-.175	.056	-.400	.092
	77.5	-.090	-.105	-.055	-.134	-.022	-.156	.008	-.182	.052	-.401	.089
	88.7	-.098	-.116	-.060	-.146	-.033	-.167	.005	-.190	.034	-.335	.077
0.777	0	.121	.075	-.054	-.055	-.051	-.177	-.130	-.266	-.198	-.321	-.249
	11.2	-.100	-.210	-.008	-.325	.060	-.357	.108	-.394	.152	-.403	.185
	22.4	-.116	-.204	-.044	-.322	.017	-.367	.067	-.399	.113	-.404	.153
	33.6	-.124	-.193	-.066	-.322	-.012	-.376	.035	-.404	.080	-.402	.123
	44.8	-.132	-.199	-.082	-.319	-.032	-.384	.013	-.408	.059	-.406	.106
	56.0	-.128	-.193	-.083	-.298	-.034	-.376	.010	-.411	.060	-.412	.108
	67.2	-.123	-.178	-.078	-.247	-.029	-.355	.015	-.409	.067	-.418	.112
	78.4	-.127	-.175	-.083	-.178	-.037	-.322	.008	-.408	.051	-.426	.089

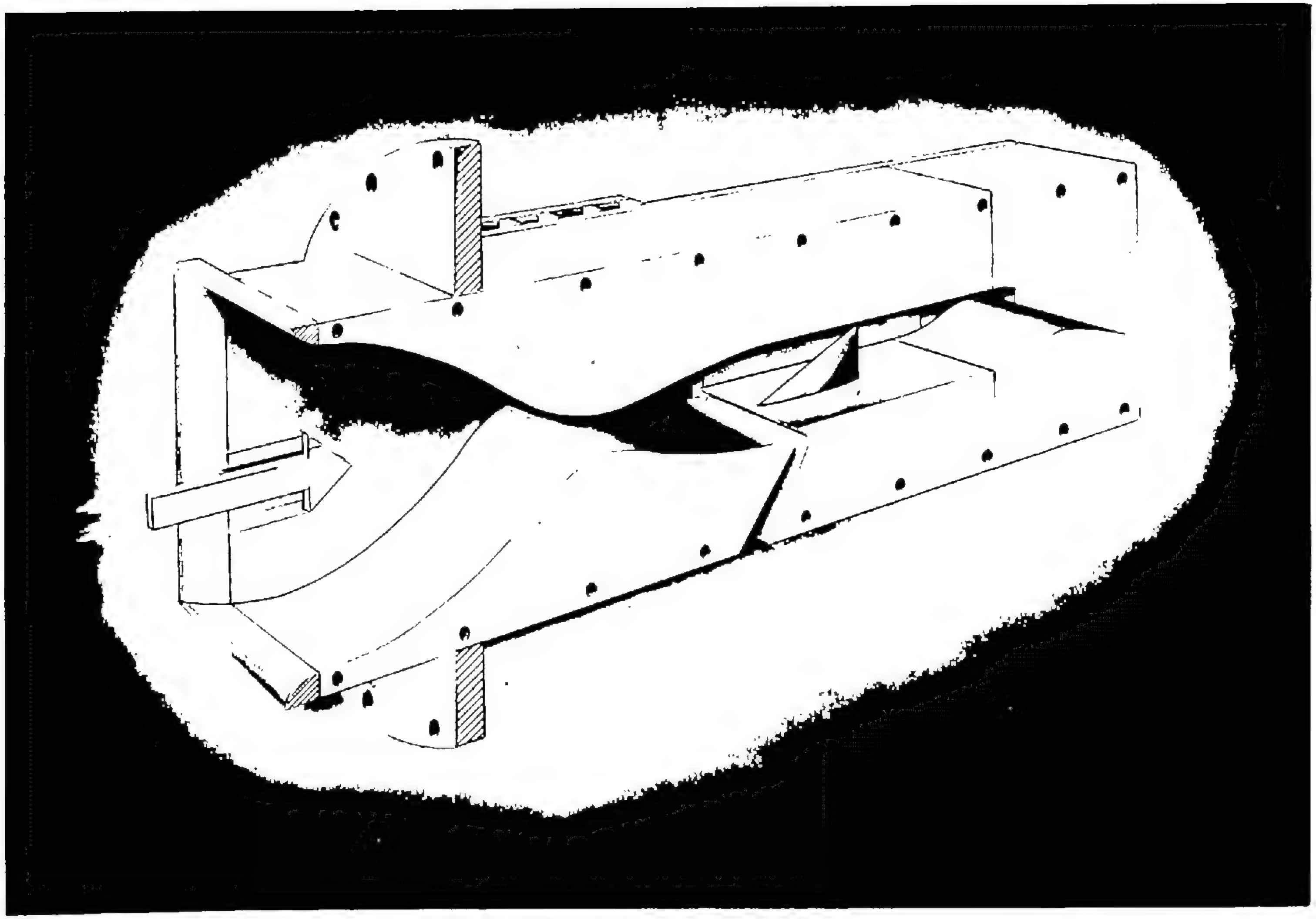

L-80472

Figure 1.- M = 1.90 blowdown jet.

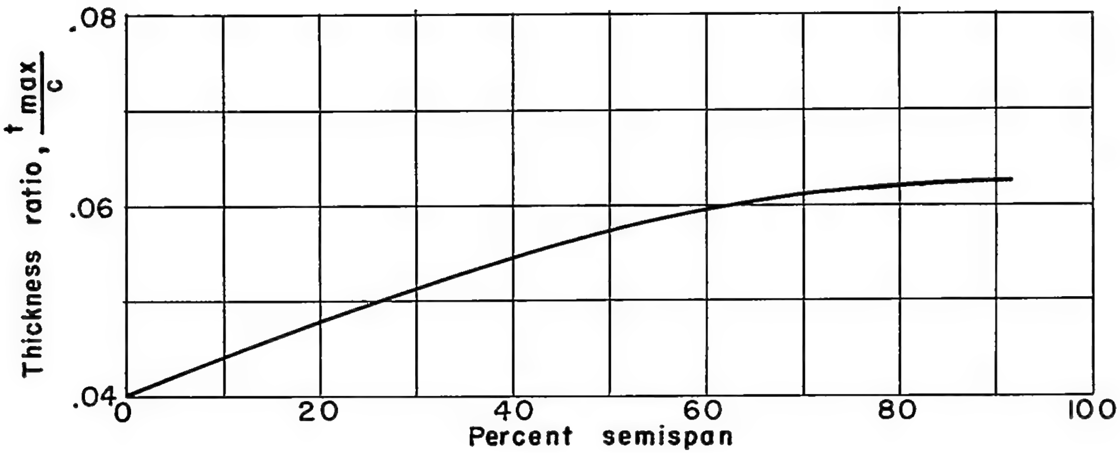

(a) Spanwise variation of maximum thickness ratio.

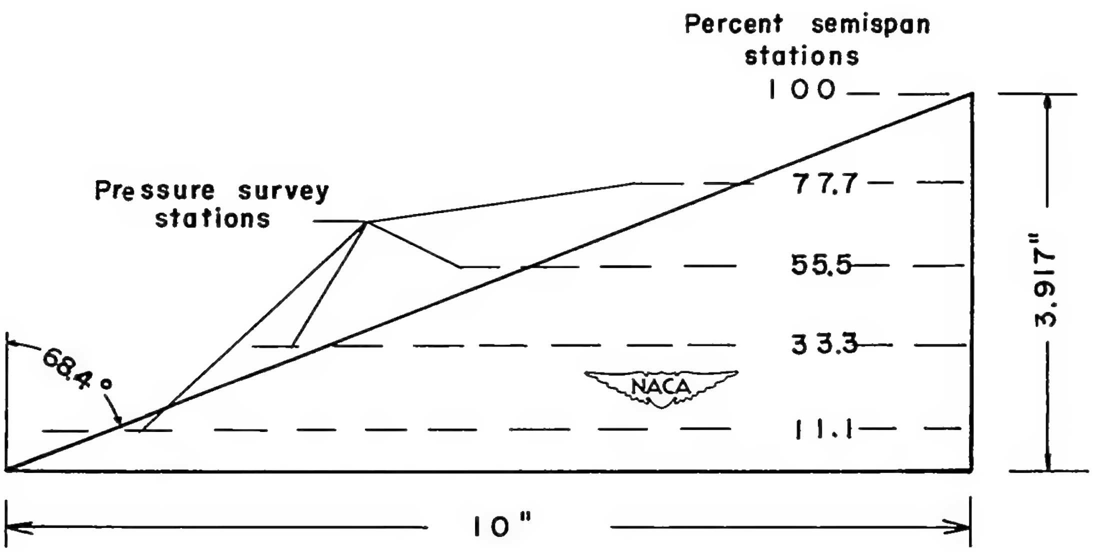

(b) Sketch of wing and pressure survey stations.

Figure 2.- Spanwise variation of maximum thickness ratio and location of pressure-survey stations.

Vane no.	Vane location	
	x/c_r	y/c_r
1	0.300	0.035
2	.300	.068
3	.300	.100
4	.500	.055
5	.500	.113
6	.500	.170
7	.700	.078
8	.700	.105
9	.700	.128
10	.700	.158
11	.700	.180
12	.700	.208
13	.700	.235
14	.900	.100
15	.900	.200
16	.900	.300

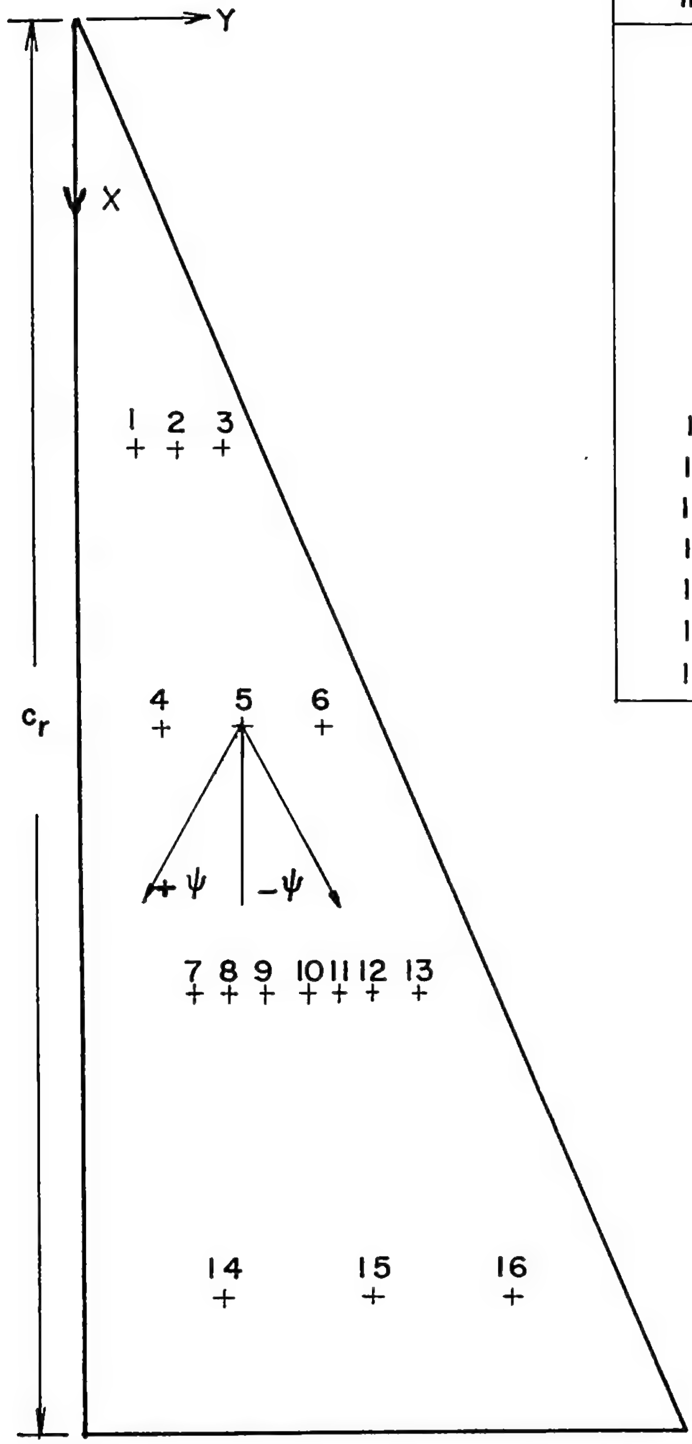

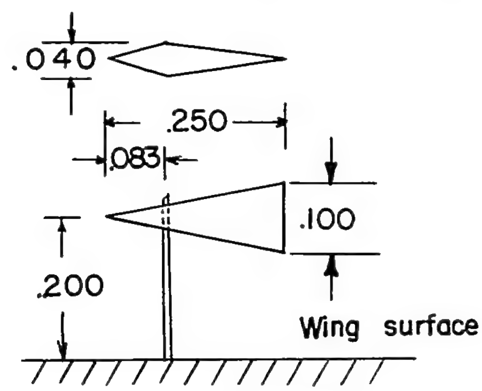

Weather cocking vane

Figure 3.- Location of flow-survey vanes on wing upper surface.

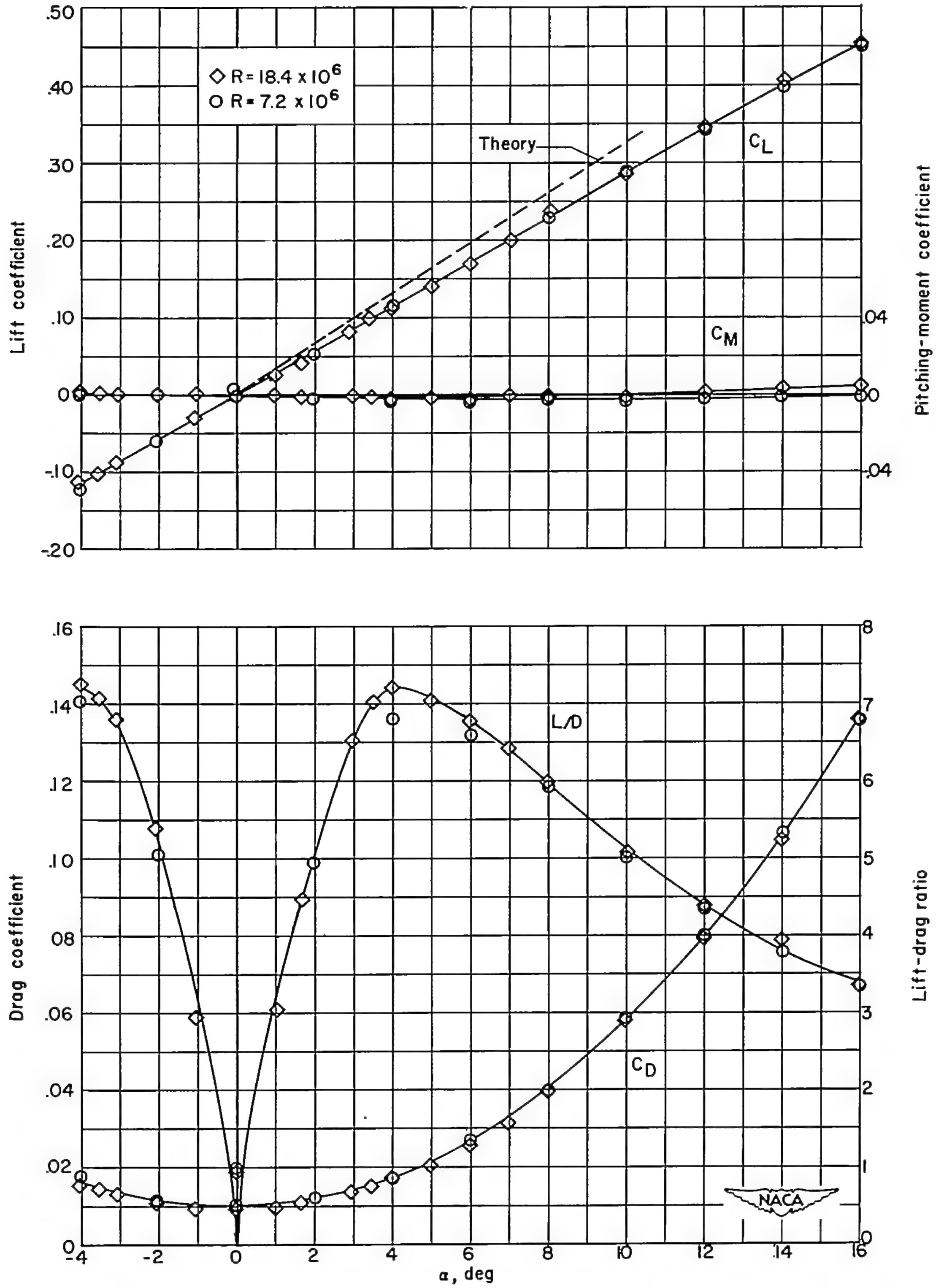

Figure 4.- Variation of wing aerodynamic characteristics with angle of attack for different Reynolds numbers. M = 1.90.

[redacted]

[redacted]

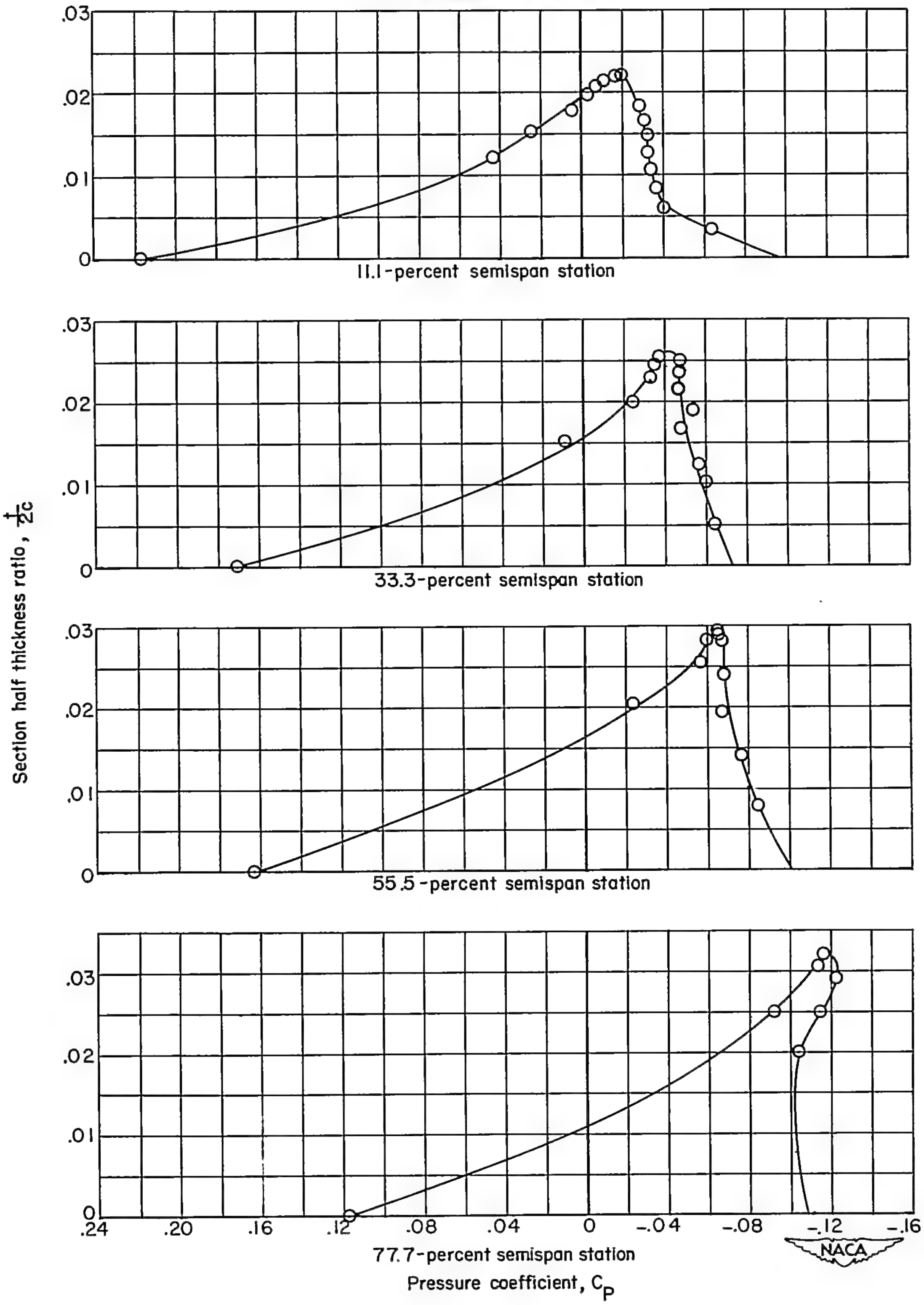

Figure 5.- Variation of pressure coefficient with thickness ratio. $M = 1.90$; $R = 18.4 \times 10^6$; $\alpha = 0^\circ$.

[redacted]

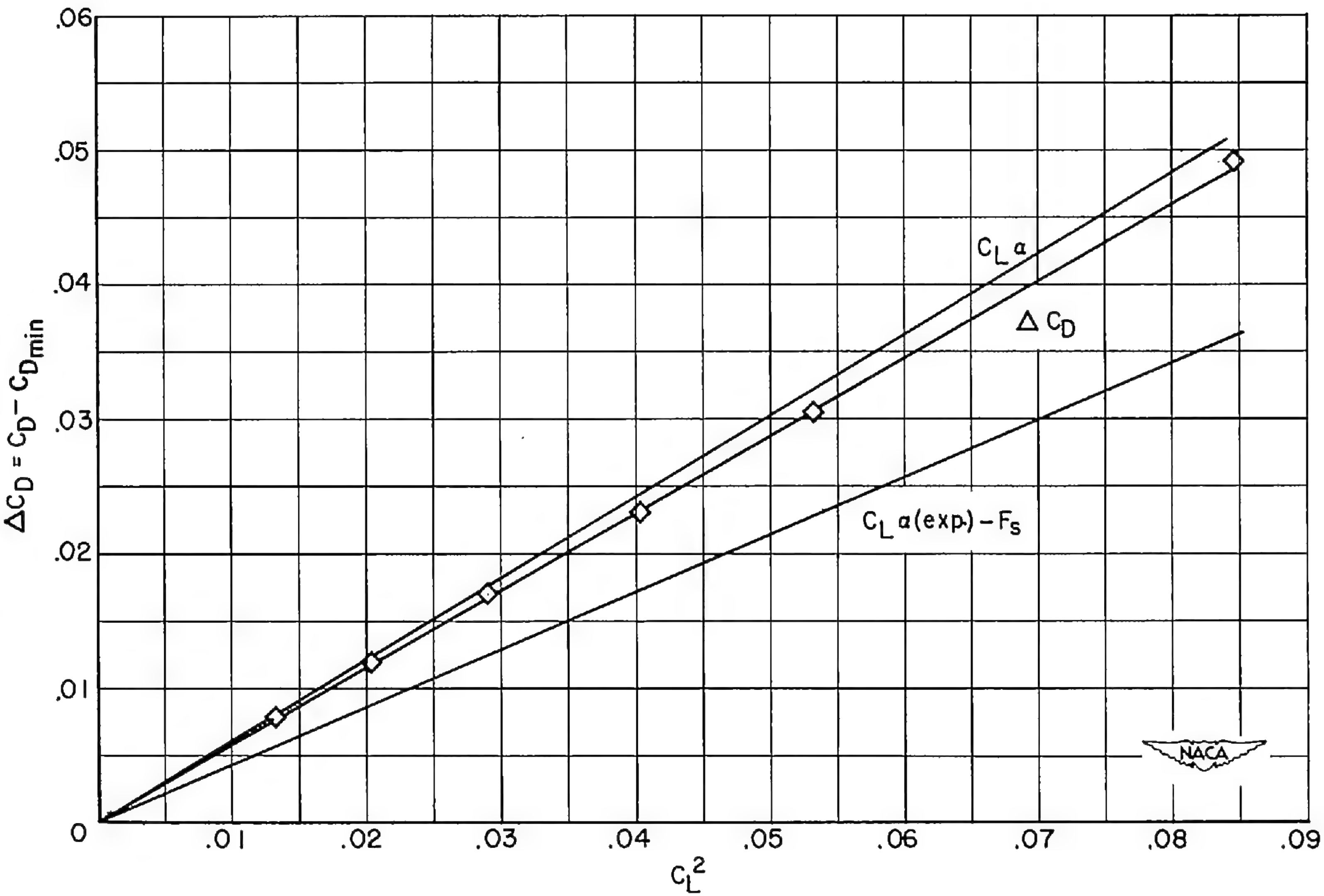

Figure 6.- Variation of ΔC_D with C_L^2. M = 1.90; R = 18.4×10^6.

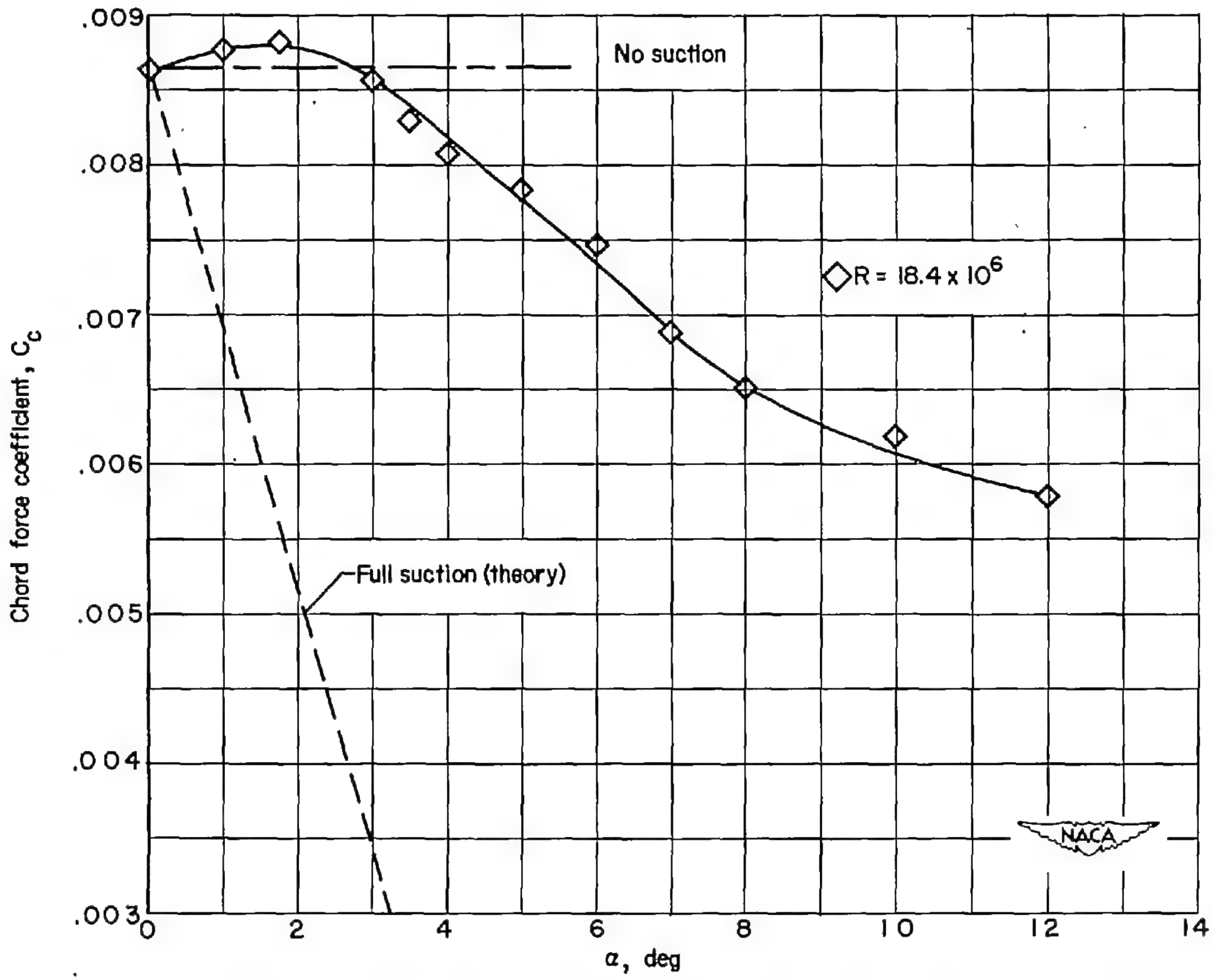

Figure 7.- Comparison of experimental and theoretical chord-force coefficients. M = 1.90.

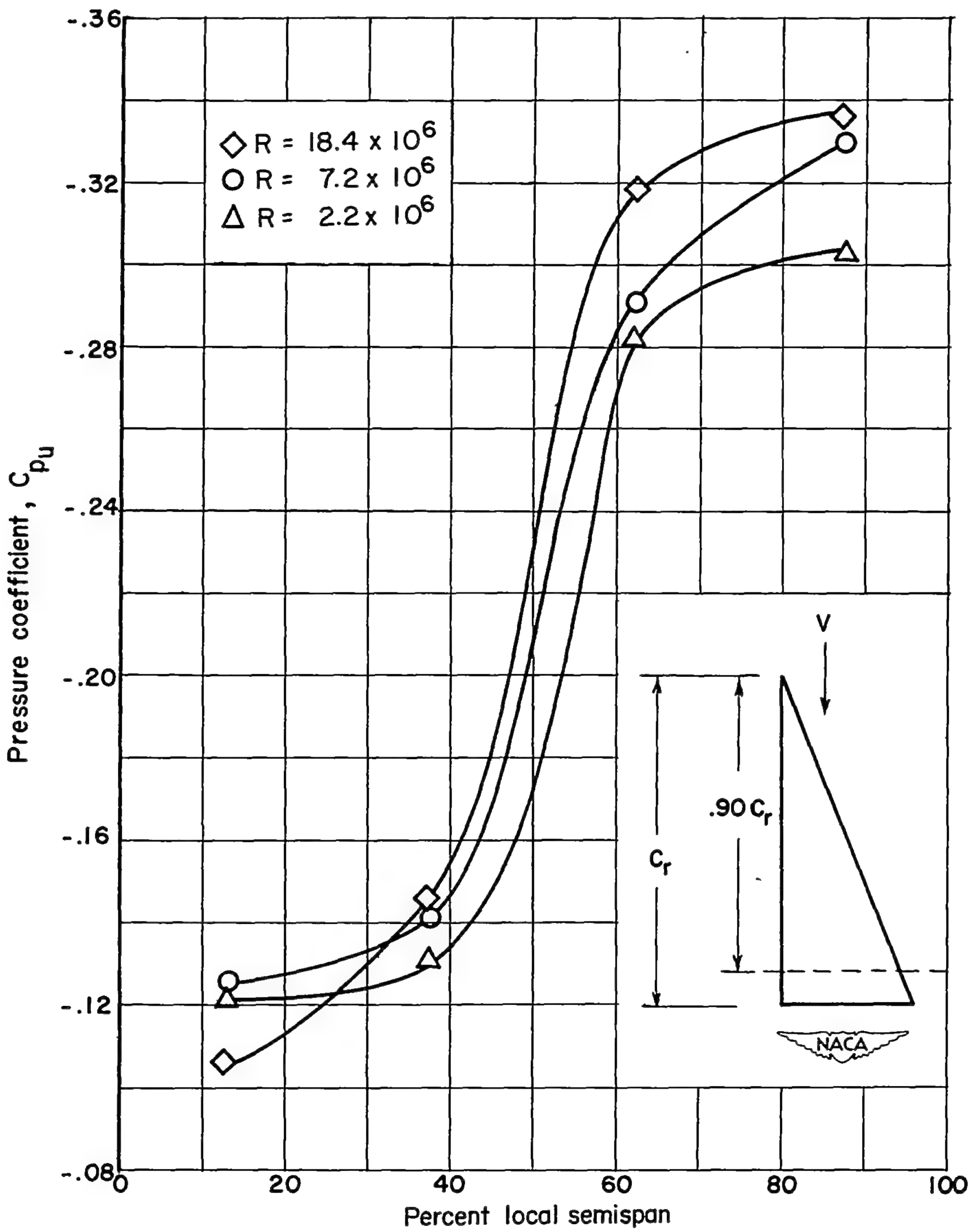

Figure 8.- Spanwise variation of upper-surface pressure coefficient at $0.90c_r$ at different Reynolds numbers. $M = 1.90$; $\alpha = 10^{\circ}$.

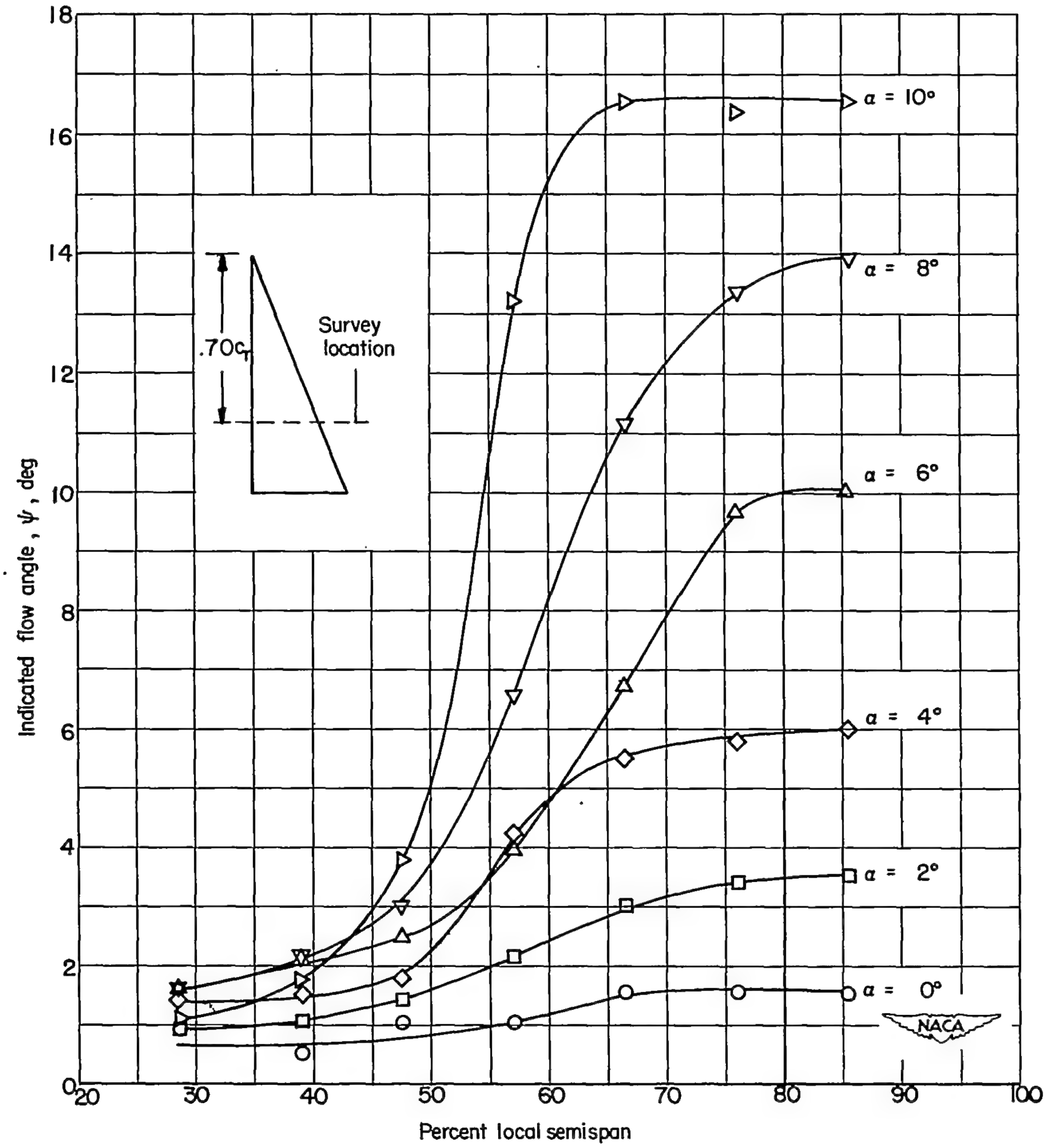

(a) M = 1.93.

Figure 9.- Measured local flow angles at $0.70c_r$ station. $R = 1.3 \times 10^6$.

[redacted]

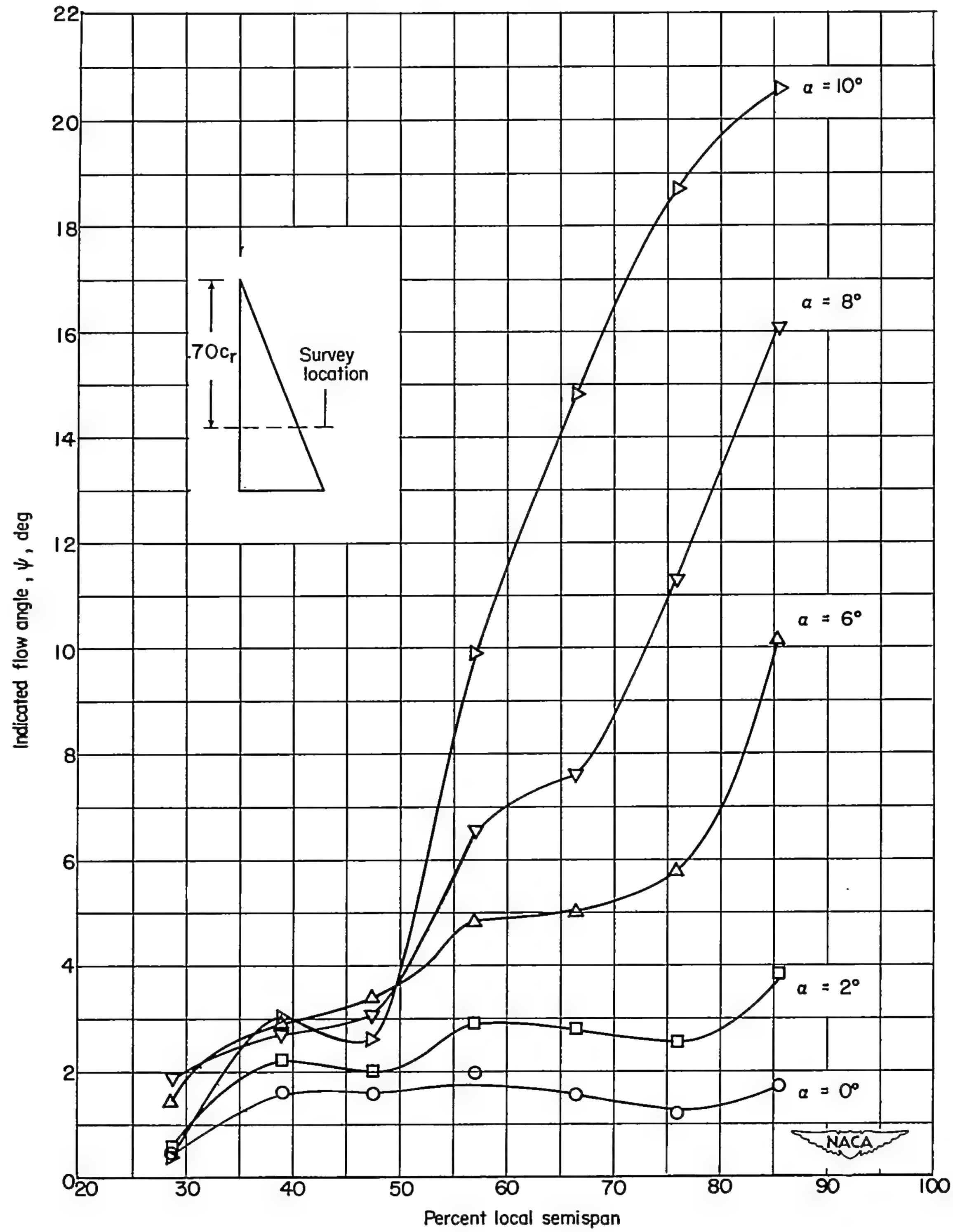

(b) M = 1.62.

Figure 9.- Concluded.

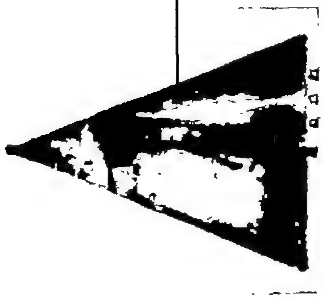

$\alpha = 0^\circ$

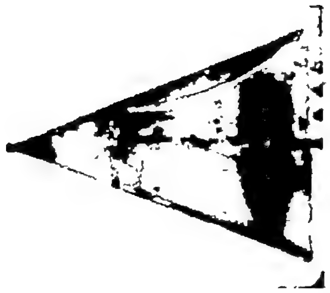

$\alpha = 2^\circ$

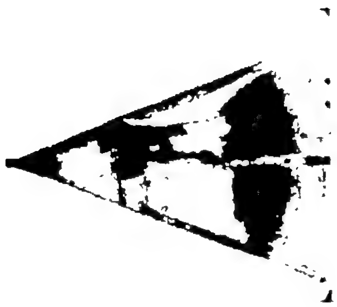

$\alpha = 4^\circ$

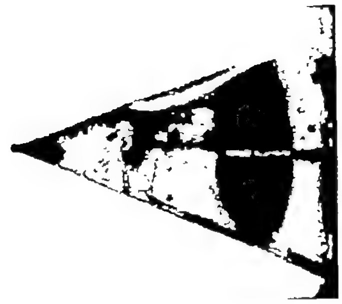

$\alpha = 6^\circ$

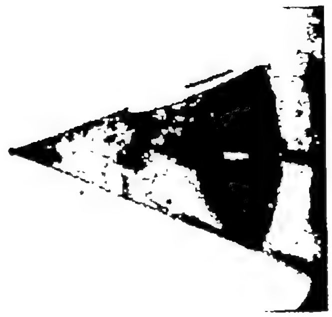

$\alpha = 8^\circ$

L-81213

Figure 10.- Ink-flow studies of boundary-layer flow on wing upper surface. Angle-of-attack effects; $R = 1.3 \times 10^6$; $M = 1.93$.

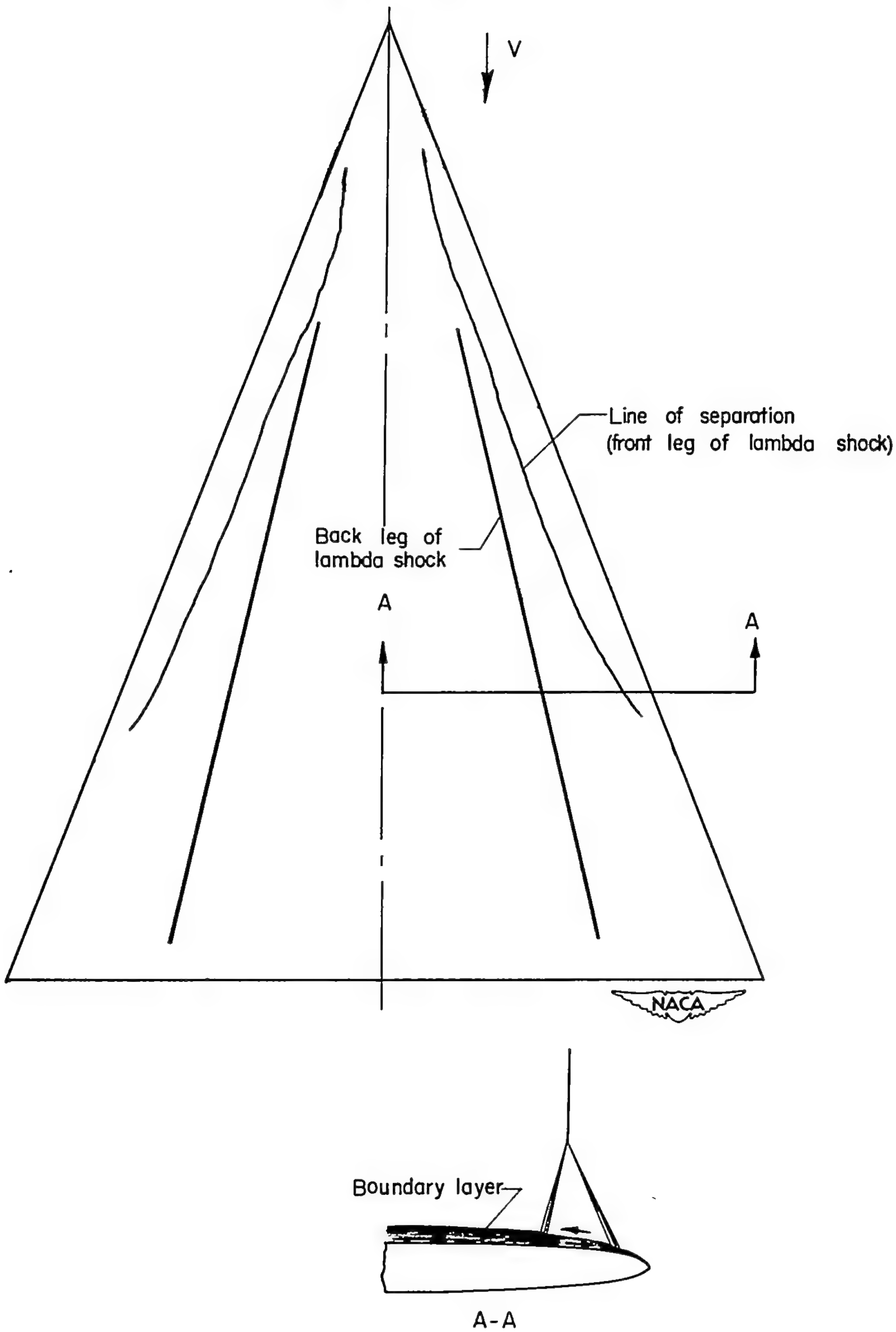

Figure 11.- Pictorial sketch of flow over the wing upper surface at moderate angles of attack. M = 1.90.

[redacted]

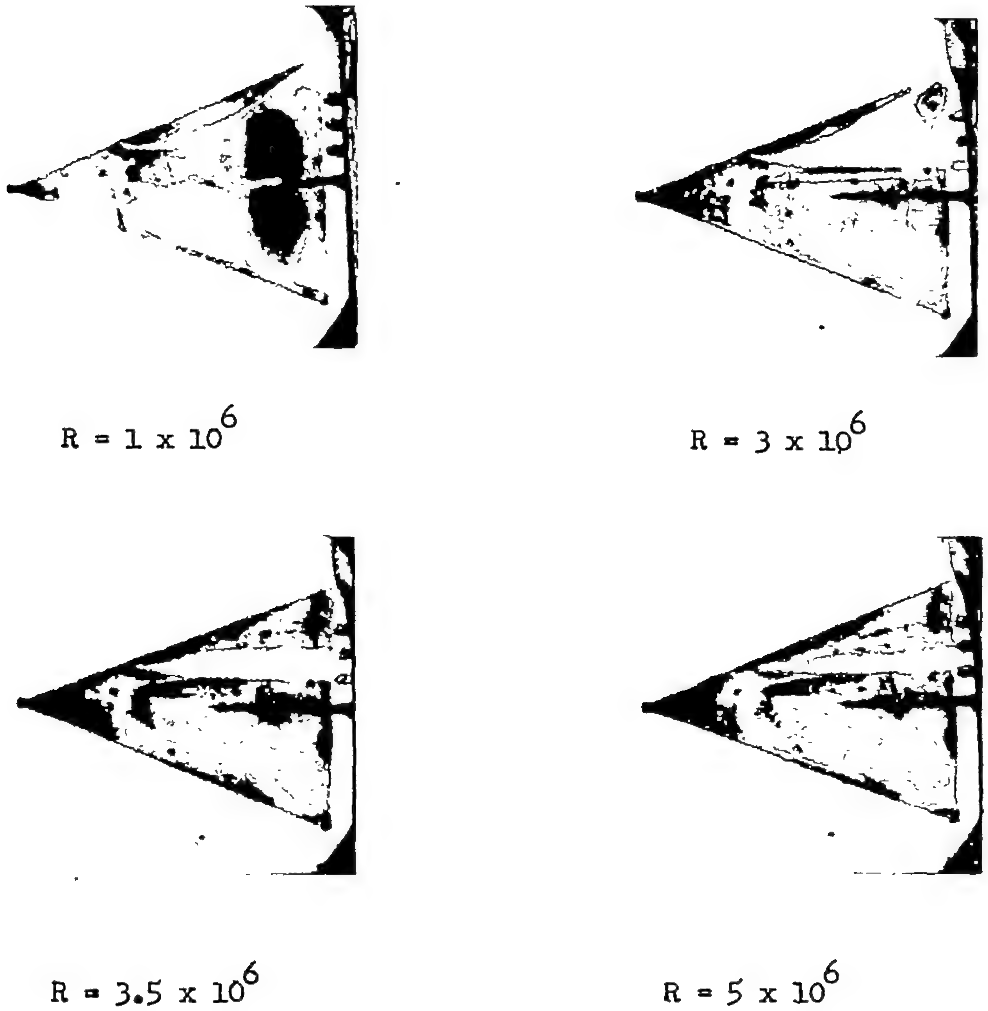

L-81214

Figure 12.- Ink-flow studies of boundary-layer flow on wing upper surface. Reynolds number effects; $\alpha = 2^{\circ}$; $M = 1.93$.

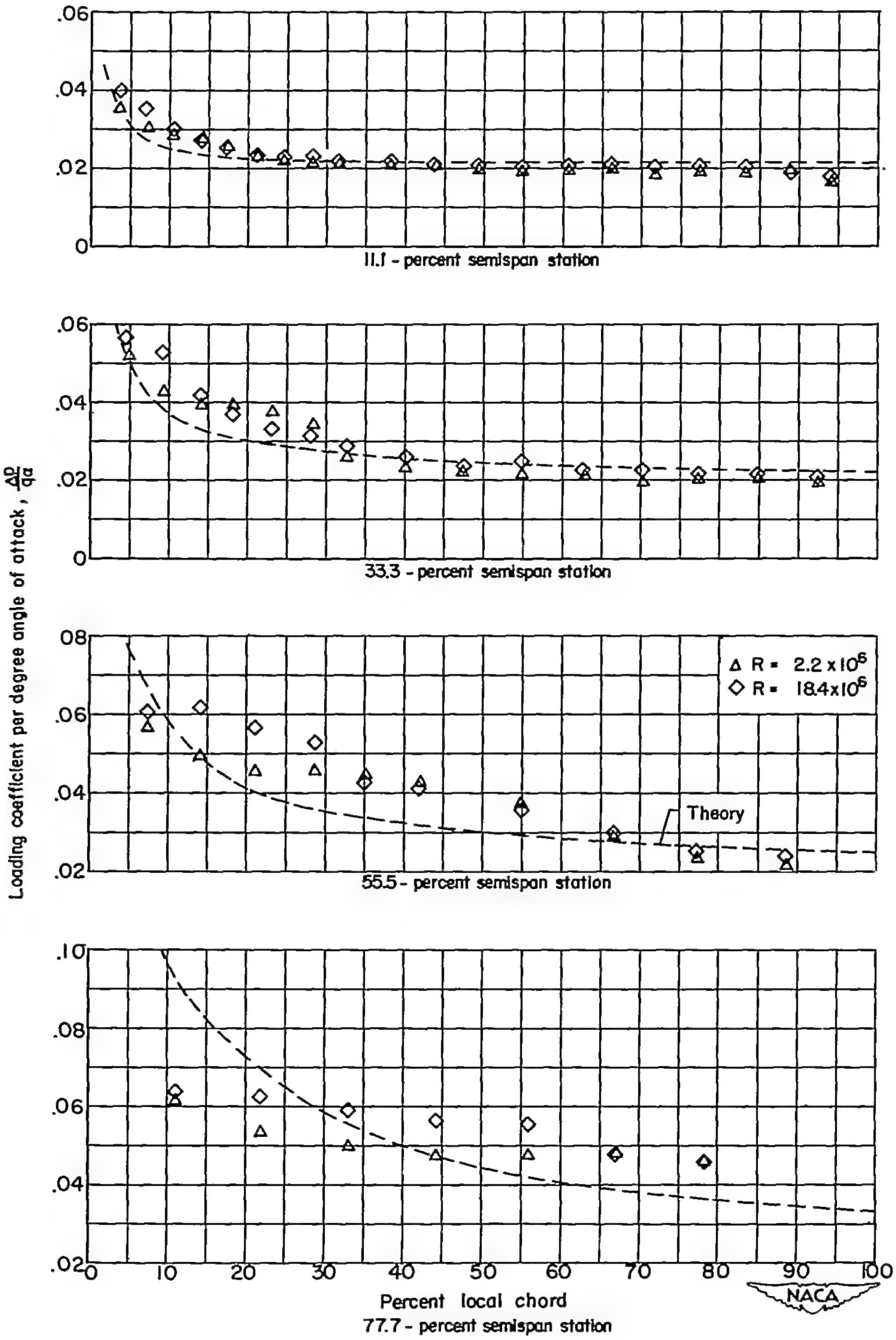

(a) M = 1.90.

Figure 13.- Chordwise variation of loading coefficients at different Reynolds numbers. $\alpha = 6^{\circ}$.

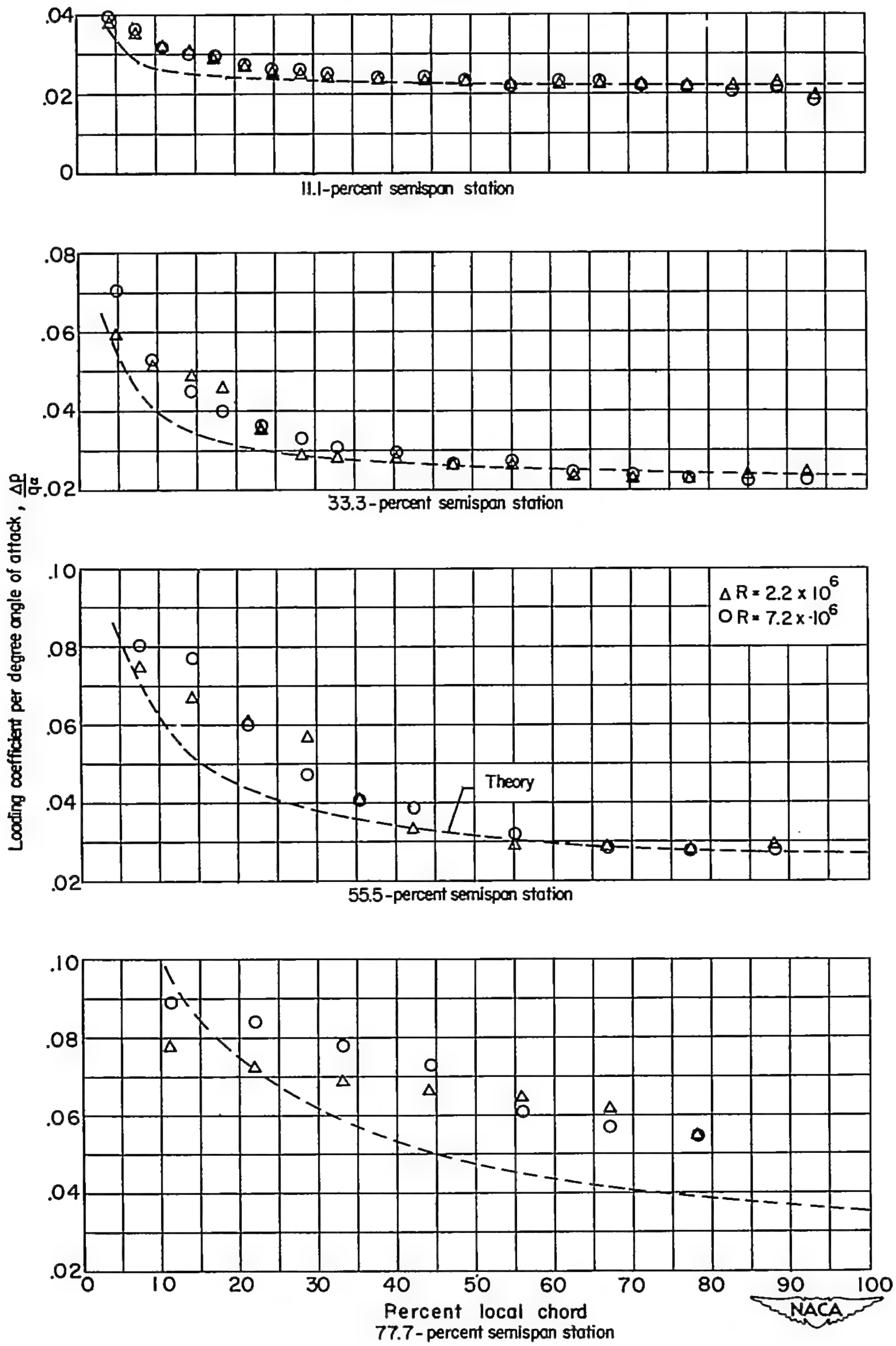

(b) M = 1.62.

Figure 13.- Concluded.

[redacted]

[redacted]

[redacted]

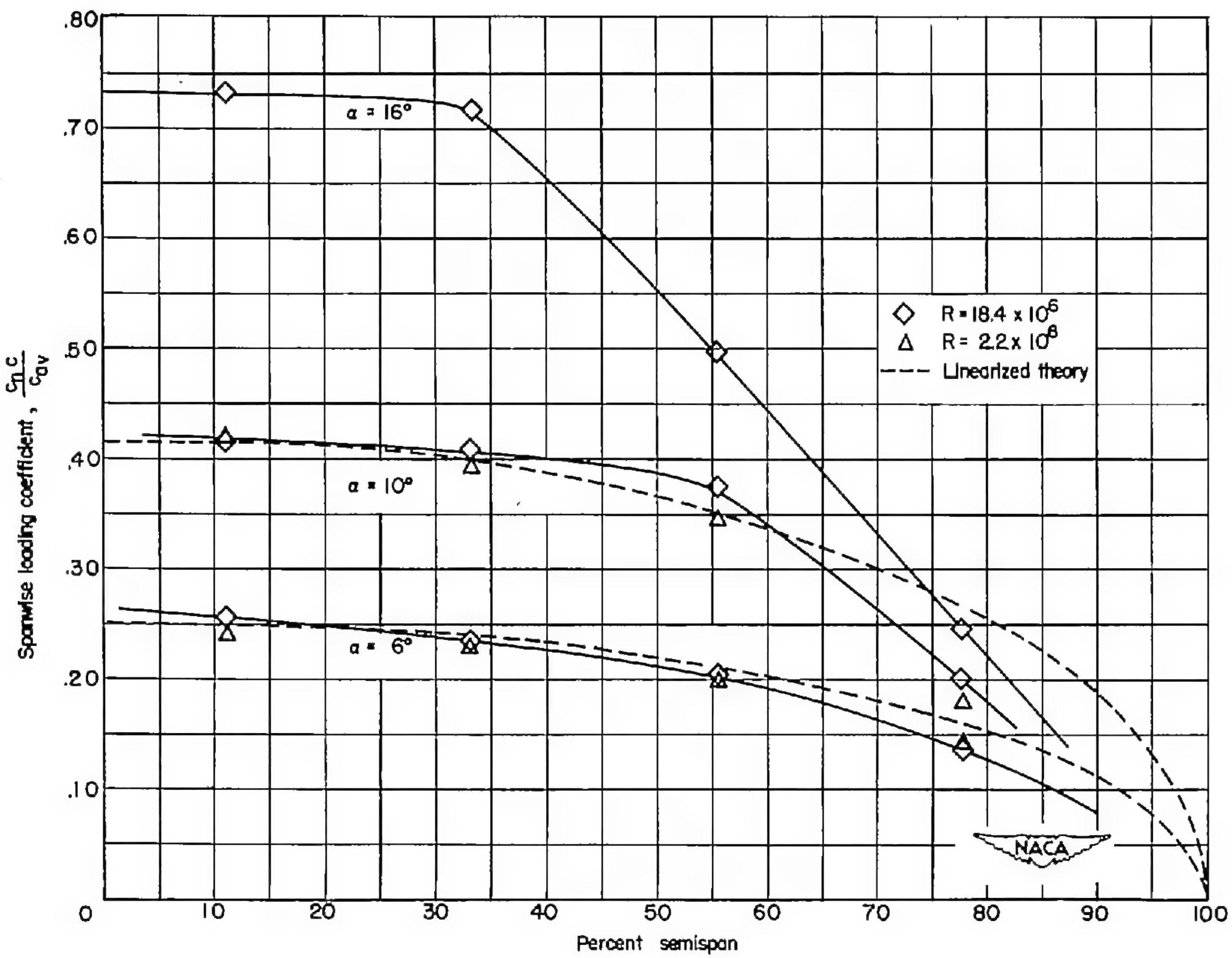

(a) M = 1.90.

Figure 14.- Spanwise load distribution at different Reynolds numbers.

[redacted]

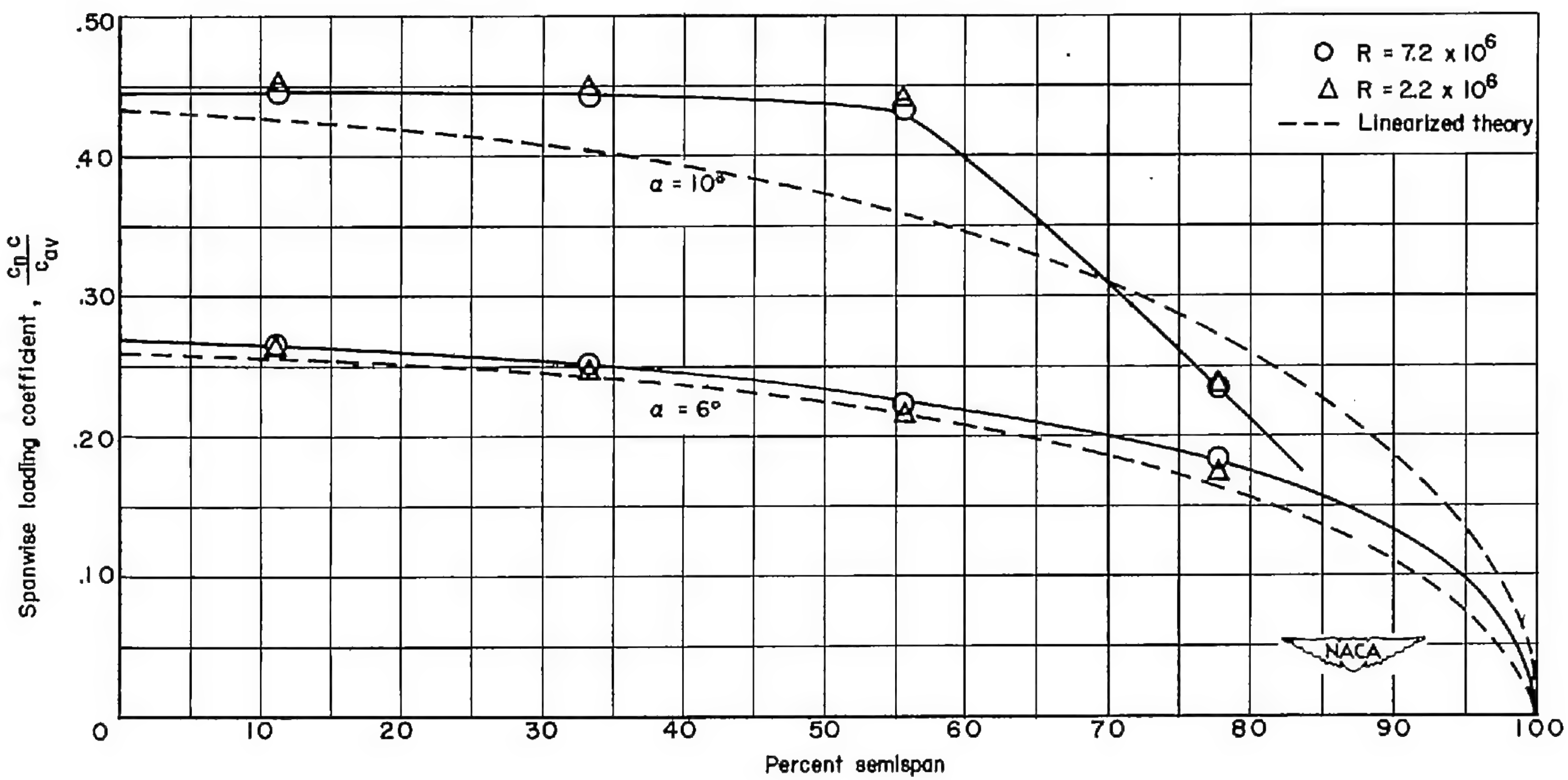

[redacted]

(b) $M = 1.62$.

Figure 14.- Concluded.

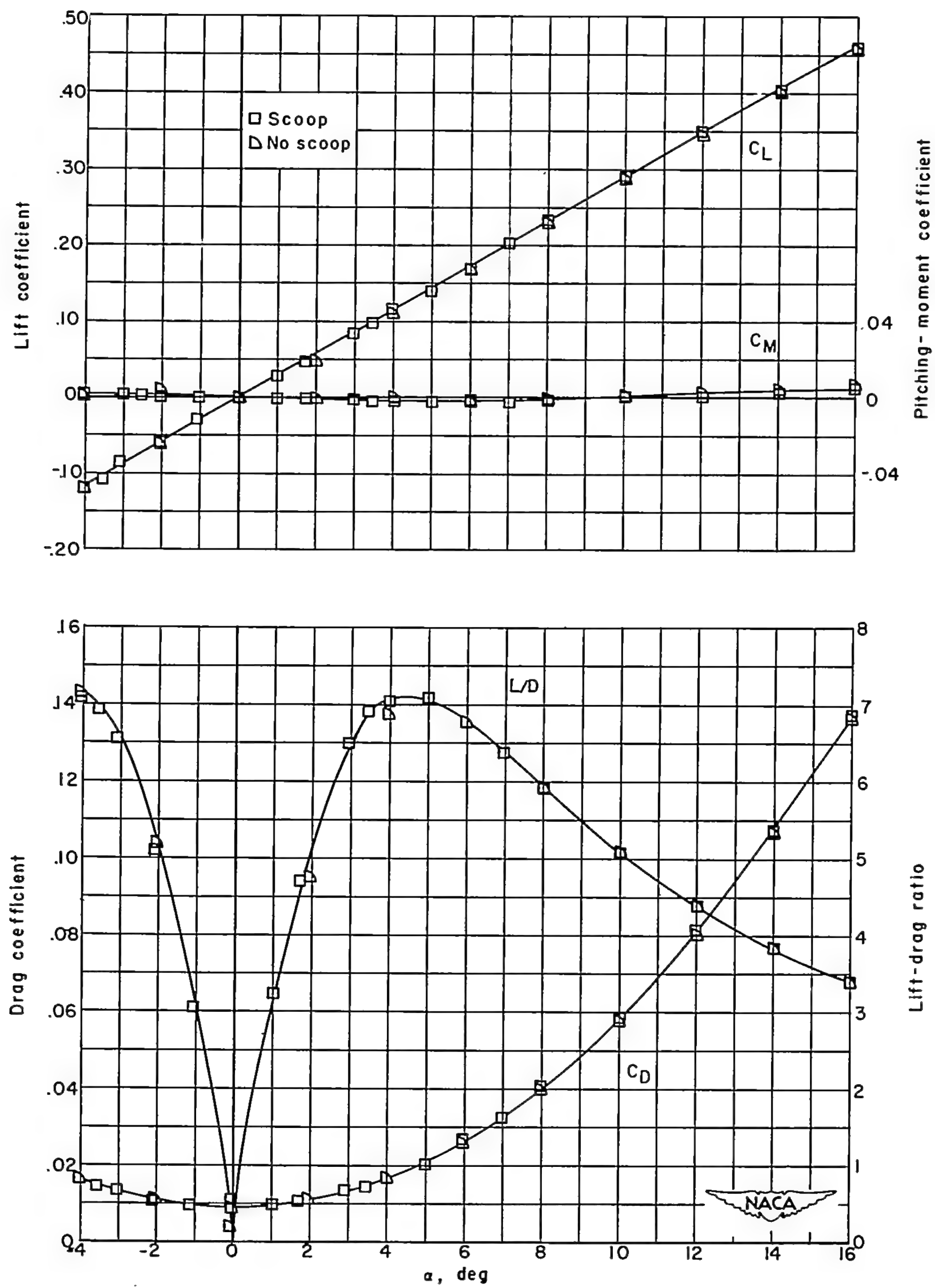

(a) M = 1.90.

Figure 15.- Variation of wing aerodynamic characteristics with angle of attack showing the effects of testing with and without a boundary-layer scoop. $R = 18.4 \times 10^6$.

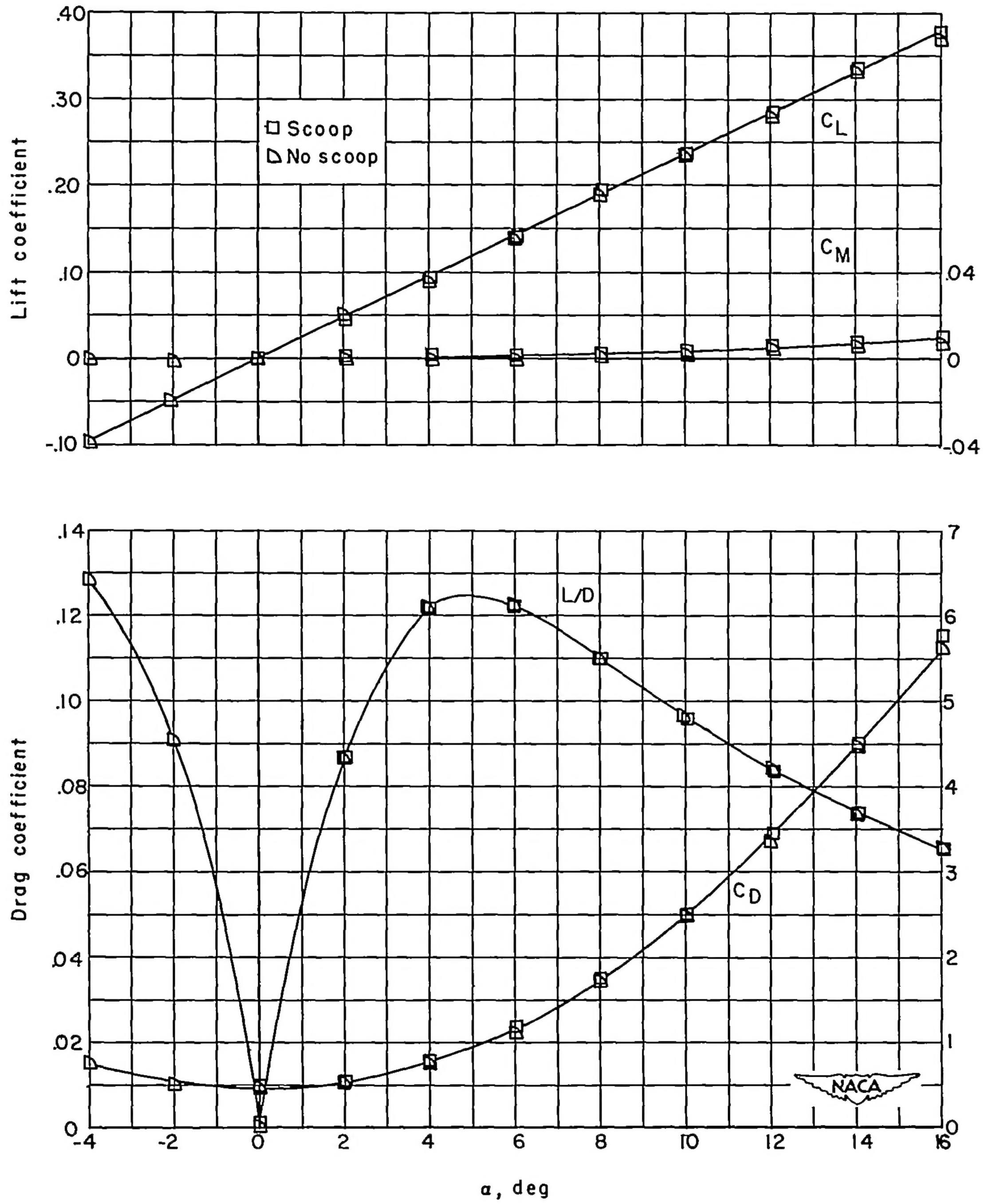

(b) $M = 2.4$; $R = 18.4 \times 10^6$.

Figure 15.- Concluded.

[redacted]

CONFIDENTIAL

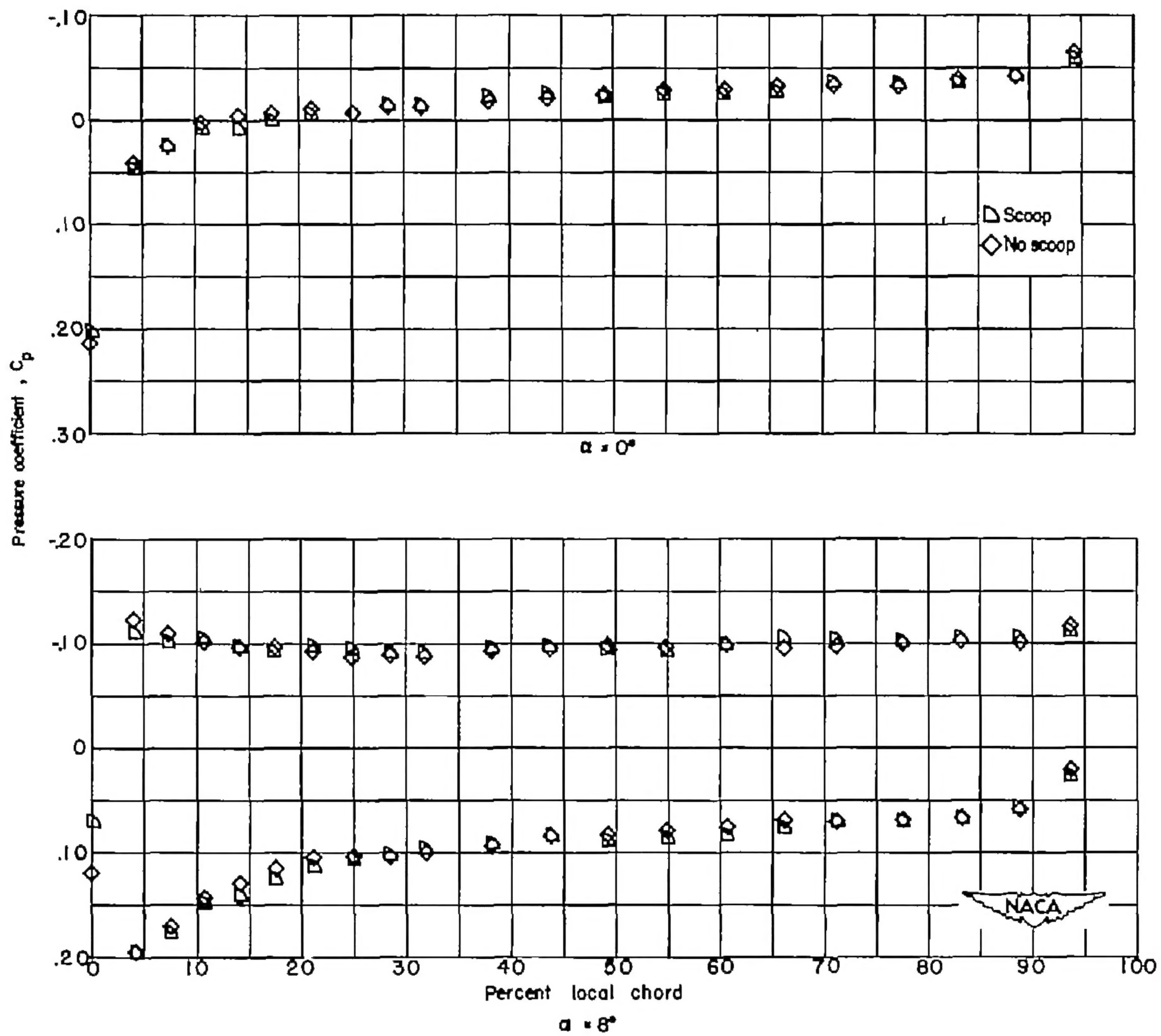

Figure 16.- Comparison of pressure distribution at 11.1-percent semispan station obtained with and without boundary-layer scoop. M = 1.90; R = 18.4 × 10^6.

CONFIDENTIAL

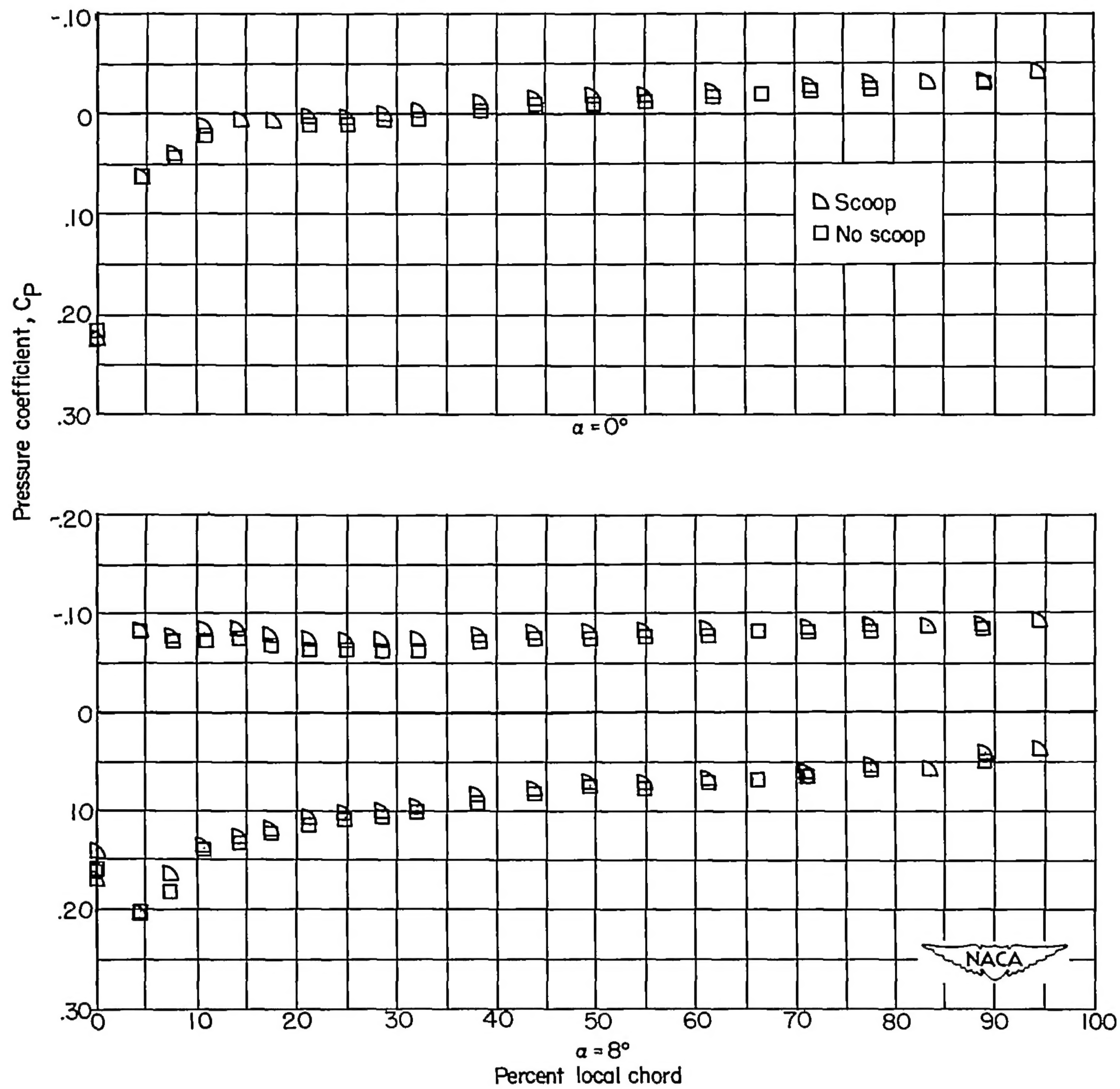

(a) 11.1-percent semispan station.

Figure 17.- Comparison of pressure distributions obtained with and without boundary-layer scoop. $M = 2.41$; $R = 18.4 \times 10^6$.

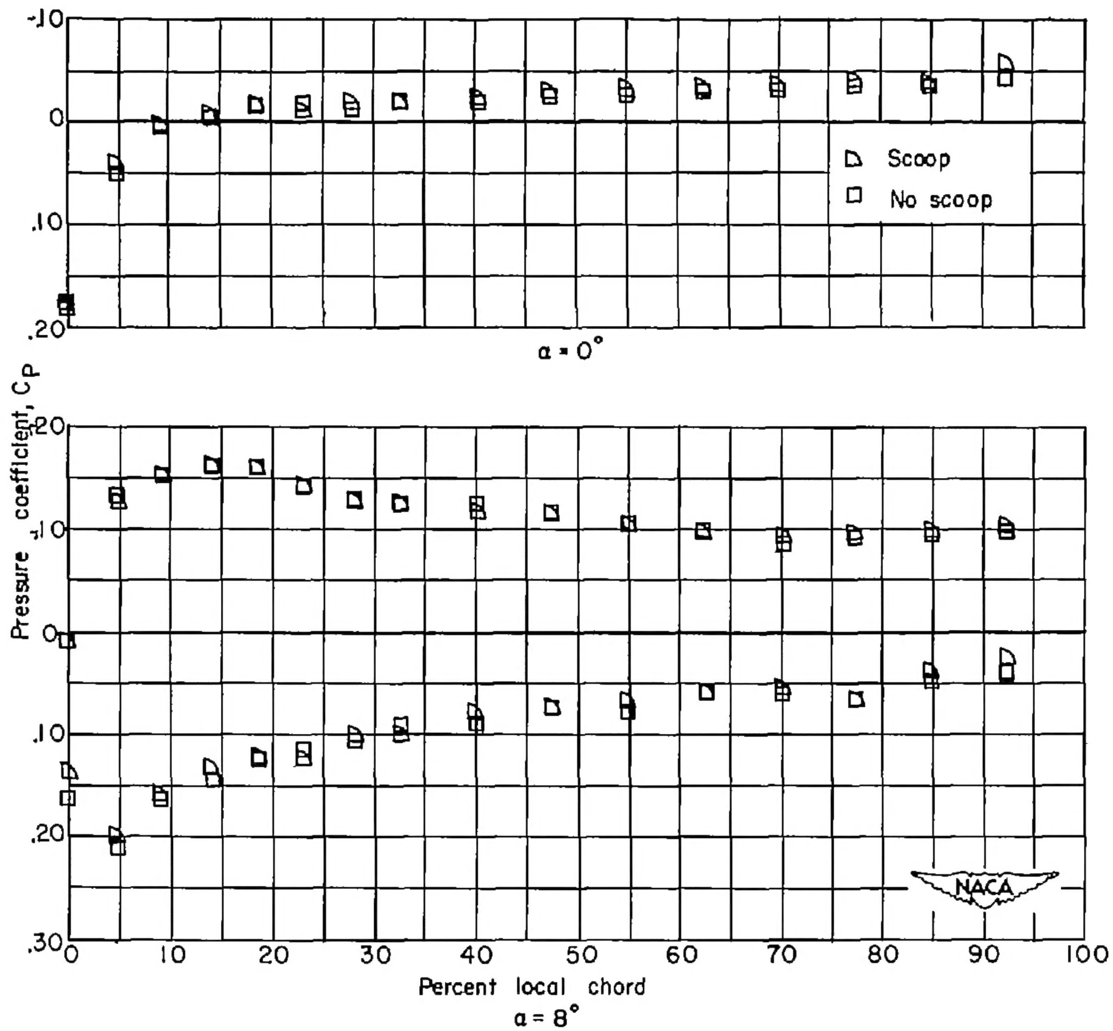

(b) 33.3 semispan station.

Figure 17.- Concluded.

NACA-Langley - 11-2-53 - 325